

Independent Component Analysis by Robust Distance Correlation

Sarah Leyder¹, Jakob Raymaekers¹, Peter J. Rousseeuw²,
Tom Van Deuren¹, and Tim Verdonck¹

¹*Department of Mathematics, University of Antwerp, Belgium*

²*Section of Statistics and Data Science, Department of Mathematics, KU Leuven, Belgium*

May 14, 2025

Abstract

Independent component analysis (ICA) is a powerful tool for decomposing a multivariate signal or distribution into truly independent sources, not just uncorrelated ones. Unfortunately, most approaches to ICA are not robust against outliers. Here we propose a robust ICA method called RICA, which estimates the components by minimizing a robust measure of dependence between multivariate random variables. The dependence measure used is the distance correlation (dCor). In order to make it more robust we first apply a new transformation called the bowl transform, which is bounded, one-to-one, continuous, and maps far outliers to points close to the origin. This preserves the crucial property that a zero dCor implies independence. RICA estimates the independent sources sequentially, by looking for the component that has the smallest dCor with the remainder. RICA is strongly consistent and has the usual parametric rate of convergence. Its robustness is investigated by a simulation study, in which it generally outperforms its competitors. The method is illustrated on three applications, including the well-known cocktail party problem.

1 Introduction

Independent component analysis (ICA) is a popular and powerful technique in statistical signal processing, originating from the work of Ans et al. (1985) and Comon (1994); for a review see

the book of Hyvärinen et al. (2001). ICA bears a superficial resemblance to principal component analysis (PCA), but there are important differences. The goal of PCA is to rotate the coordinate axes to obtain a coordinate system in which the variables become uncorrelated. The new variables are then called principal components, after which one may reduce the data dimension by keeping only the principal components with the highest variance. On the other hand, ICA looks for a coordinate system in which the variables, called *sources*, are independent. This is quite different because uncorrelated variables are not necessarily independent, so for ICA it does not suffice to know the covariance matrix of the data. Another crucial difference is that ICA allows to transform the coordinate axes by a general linear transformation, whereas PCA was restricted to orthogonal transformations. Because the dependence structure of a multivariate Gaussian distribution is fully determined by its nonsingular covariance matrix, which can be turned into any other positive definite matrix by a linear data transformation, ICA can only detect non-Gaussian independent components.

Taken together, the above aspects make ICA more complex than PCA. But it has many important applications in statistics and engineering. Several methodological tools depend on ICA, including blind source separation (Cardoso, 1998; Comon and Jutten, 2010), causal discovery (Shimizu et al., 2006), feature extraction, preprocessing, artifact removal, and noise reduction. Tools based on ICA have been applied across various fields such as biomedical sciences, audio and image preprocessing, biometrics, and finance. For application overviews see e.g. Tharwat (2021) and Naik and Kumar (2011). In such applications the independent sources often have natural interpretations. In Section 6 we will illustrate this with image data, audio data, and periodic data.

The basic formulation of the ICA setting goes as follows. Suppose we observe n i.i.d. observations $\mathbf{x}_1, \dots, \mathbf{x}_n$ which are realizations of a d -dimensional random vector \mathbf{X} . We denote the $n \times d$ data matrix by \mathbf{X}_n . The independent component model assumes that the random vector \mathbf{X} can be written as

$$\mathbf{X} = \mathbf{AS} \tag{1}$$

where \mathbf{S} is an unobserved d -variate non-Gaussian random vector whose components are mutually independent. Here \mathbf{A} is an unknown non-singular $d \times d$ matrix, called the *mixing matrix*. Only the linear mixture \mathbf{X} is observable, whereas \mathbf{A} and \mathbf{S} are both unknown. Given the data $\mathbf{x}_1, \dots, \mathbf{x}_n$, the goal of ICA is to estimate the mixing matrix $\hat{\mathbf{A}}$ which can then be used to “unmix” the observed \mathbf{x}_i by computing $\mathbf{s}_i = \hat{\mathbf{A}}^{-1} \mathbf{x}_i$ for $i = 1, \dots, n$. Note that the scale, sign and order of the components of \mathbf{S} are not identifiable from the distribution of \mathbf{X} . Therefore we aim to recover \mathbf{A}

up to multiplication by a signed permutation matrix and a diagonal scale matrix.

Several generalizations of the model (1) exist. For instance, some consider a “noisy” version which adds some extra Gaussian noise to \mathbf{X} , see e.g. Voss et al. (2015). Other generalizations allow some of the components in \mathbf{S} to be Gaussian, and target the identification of the non-Gaussian components only (Nordhausen and Oja, 2018).

Various approaches exist for separating the mixed sources that created \mathbf{X} . A first set of algorithms uses measures of non-Gaussianity to extract \mathbf{S} , such as kurtosis or approximations of negentropy (Hyvärinen and Oja, 1997; Hyvärinen, 1999), resulting in the renowned FastICA algorithm of Hyvärinen and Oja (2000). A second approach for extracting the independent sources is to maximize entropy, as done by the infomax (Bell and Sejnowski, 1995) and extended infomax (Lee et al., 1999) methods. A third approach for recovering the independent sources is to jointly diagonalize fourth order cumulants, resulting in the JADE algorithm of Cardoso and Souloumiac (1993); Miettinen et al. (2015).

Although these ICA methods have demonstrated success and broad applicability, they generally exhibit a high sensitivity to outliers. One reason is that classical statistical estimators of kurtosis and higher-order cumulants are known to be heavily influenced by outliers. The effect of outliers on an estimator can be measured by its influence function (Hampel et al., 1986), which ideally should be bounded. But FastICA has an unbounded influence function, regardless of the chosen contrast function (Hyvärinen, 1999; Ollila, 2009; Nordhausen et al., 2011a). The issue is that outliers can generate new dependencies that violate the underlying independent component model. Therefore we cannot expect to recover the sources perfectly, but we can try to construct a more robust ICA method that mitigates the bias caused by outliers as much as possible.

Some studies have addressed the robustness of ICA algorithms. Hyvärinen (1999) analyzed the statistical properties of different contrast functions within the FastICA algorithm, leading to recommendations to achieve more robustness. While kurtosis is very sensitive to outliers, he proposed bounded alternative contrast functions, thereby reducing the effect of extreme values. These findings were supported by a simulation study. Building on this, Brys et al. (2005) extended FastICA by adding a preprocessing step using an outlier rejection rule. This removes gross outliers, but makes the method less efficient when the data is not contaminated by outliers. Learned-Miller and Fisher (2003) proposed the RADICAL method based on a nonparametric entropy estimator. While certainly more robust than FastICA, the robustness of RADICAL deteriorates substantially with increasing dimension and number of outliers. Chen et al. (2013) proposed a robust approach to ICA using γ -divergence. Their method, termed γ -ICA, aims to leverage the robustness properties

of γ -divergence against outliers, and is consistent when the components of \mathbf{S} are symmetrically distributed. However, γ -ICA requires the selection of the tuning parameter γ , and the empirical evaluation of its robustness was somewhat limited.

In this work we propose a new robust ICA method. It is based on the dCovICA method of Matteson and Tsay (2017), which minimizes the dependence between the recovered signals. For this purpose it measures dependence by the distance covariance of Székely et al. (2007). Although this measure of dependence offers some inherent resistance against outliers, it was recently shown in (Leyder et al., 2024a) that its robustness against increasing numbers of gross outliers can be improved. This was achieved by subjecting the data to a new type of transformation before computing the distance covariance. In the current paper we extend this approach from univariate to multivariate variables. We then use it to construct RICA, a **Robust ICA** procedure, which operates by minimizing this robust dependence measure between a potential new source and the remainder.

The paper is structured as follows. Section 2 introduces some preliminary concepts needed to construct RICA. Section 3 provides a detailed description of the RICA methodology. Next, Section 4 formulates theoretical properties of the method. The extensive simulation results presented in Section 5 demonstrate the enhanced robustness of RICA against outliers. Section 6 showcases some examples on real datasets, and Section 7 concludes.

2 Preliminaries

We first introduce the background concepts on which we build our proposal.

2.1 Whitening

The problem of identifying the *unmixing matrix* \mathbf{A}^{-1} in the ICA problem can be simplified somewhat by first decorrelating the observed data \mathbf{X}_n . This process is known as “whitening”. For this one typically constructs a nonsingular $d \times d$ matrix \mathbf{W} such that $\mathbf{Z} = \mathbf{W}\mathbf{X}$ has uncorrelated components with unit variances, i.e. $\text{Cov}(\mathbf{Z}) = \mathbf{I}$. Then we can write

$$\mathbf{S} = \mathbf{A}^{-1}\mathbf{X} = \mathbf{A}^{-1}\mathbf{W}^{-1}\mathbf{Z} = \mathbf{U}\mathbf{Z},$$

where $\mathbf{U} = \mathbf{A}^{-1}\mathbf{W}^{-1}$ is called the *separating matrix*. Let us assume without loss of generality that $\text{Cov}(\mathbf{S}) = \mathbf{I}$. Then the separating matrix is an orthogonal matrix because

$$\mathbf{I} = \text{Cov}(\mathbf{S}) = \mathbf{U}\text{Cov}(\mathbf{Z})\mathbf{U}^T = \mathbf{U}\mathbf{U}^T.$$

Orthogonal $d \times d$ matrices only have $d(d - 1)/2$ free elements instead of d^2 , as will be described in Section 3.3. Therefore whitening reduces the dimension of the search space for \mathbf{U} to roughly half of the size of the unmixing matrix \mathbf{A}^{-1} .

2.2 Distance covariance and correlation

The distance covariance (dCov) was introduced by Székely et al. (2007) as a measure of general dependence between random vectors. For random vectors \mathbf{X} and \mathbf{Y} with finite second moments it is defined as

$$\text{dCov}(\mathbf{X}, \mathbf{Y}) = \mathbb{E}[||\mathbf{X} - \mathbf{X}'|| ||\mathbf{Y} - \mathbf{Y}'||] + \mathbb{E}[||\mathbf{X} - \mathbf{X}'||] \mathbb{E}[||\mathbf{Y} - \mathbf{Y}'||] - 2\mathbb{E}[||\mathbf{X} - \mathbf{X}'|| ||\mathbf{Y} - \mathbf{Y}''||],$$

where $(\mathbf{X}', \mathbf{Y}')$ is an independent copy of (\mathbf{X}, \mathbf{Y}) , \mathbf{Y}'' is another independent copy of \mathbf{Y} , and $|| . ||$ is the Euclidean norm. The distance covariance is a measure of dependence that is always nonnegative, and it is zero if and only if the random vectors are independent:

$$\text{dCov}(\mathbf{X}, \mathbf{Y}) = 0 \iff \mathbf{X} \perp\!\!\!\perp \mathbf{Y},$$

where $\perp\!\!\!\perp$ stands for ‘‘independent of’’. The arrow \Leftarrow holds for the usual covariance as well, but definitely not the arrow \Rightarrow that is the main strength of dCov.

Székely et al. (2007) also defined the *distance variance*, *distance standard deviation*, and *distance correlation*, given by

$$\begin{aligned}\text{dVar}(\mathbf{X}) &= \text{dCov}(\mathbf{X}, \mathbf{X}) \\ \text{dStd}(\mathbf{X}) &= \sqrt{\text{dVar}(\mathbf{X})} \\ \text{dCor}(\mathbf{X}, \mathbf{Y}) &= \frac{\text{dCov}(\mathbf{X}, \mathbf{Y})}{\text{dStd}(\mathbf{X})\text{dStd}(\mathbf{Y})}.\end{aligned}$$

The distance correlation dCor has the nice property that it always lies in the interval $[0, 1]$. This makes it more easily interpretable than dCov, which depends on the magnitude and units of the data. The empirical distance covariance of multivariate datasets $(\mathbf{X}_n, \mathbf{Y}_n)$ is given by

$$\text{dCov}_n(\mathbf{X}_n, \mathbf{Y}_n) = T_{1,n}(\mathbf{X}_n, \mathbf{Y}_n) + T_{2,n}(\mathbf{X}_n, \mathbf{Y}_n) - T_{3,n}(\mathbf{X}_n, \mathbf{Y}_n)$$

with the following terms:

$$\begin{aligned}
T_{1,n}(\mathbf{X}_n, \mathbf{Y}_n) &= \binom{n}{2}^{-1} \sum_{i < j} \|\mathbf{x}_i - \mathbf{x}_j\| \|\mathbf{y}_i - \mathbf{y}_j\|, \\
T_{2,n}(\mathbf{X}_n, \mathbf{Y}_n) &= \left[\binom{n}{2}^{-1} \sum_{i < j} \|\mathbf{x}_i - \mathbf{x}_j\| \right] \left[\binom{n}{2}^{-1} \sum_{i < j} \|\mathbf{y}_i - \mathbf{y}_j\| \right], \\
T_{3,n}(\mathbf{X}_n, \mathbf{Y}_n) &= \binom{n}{3}^{-1} \sum_{i < j < k} \left[\|\mathbf{x}_i - \mathbf{x}_j\| \|\mathbf{y}_i - \mathbf{y}_k\| + \|\mathbf{x}_i - \mathbf{x}_k\| \|\mathbf{y}_i - \mathbf{y}_j\| + \|\mathbf{x}_i - \mathbf{x}_j\| \|\mathbf{y}_j - \mathbf{y}_k\| \right. \\
&\quad \left. + \|\mathbf{x}_j - \mathbf{x}_k\| \|\mathbf{y}_i - \mathbf{y}_j\| + \|\mathbf{x}_i - \mathbf{x}_k\| \|\mathbf{y}_j - \mathbf{y}_k\| + \|\mathbf{x}_j - \mathbf{x}_k\| \|\mathbf{y}_i - \mathbf{y}_k\| \right].
\end{aligned}$$

The empirical distance variance and the distance correlation are defined similarly as

$$\begin{aligned}
\text{dVar}_n(\mathbf{X}_n) &= \text{dCov}_n(\mathbf{X}_n, \mathbf{X}_n), \\
\text{dCor}_n(\mathbf{X}_n, \mathbf{Y}_n) &= \frac{\text{dCov}_n(\mathbf{X}_n, \mathbf{Y}_n)}{\sqrt{\text{dVar}_n(\mathbf{X}_n) \text{dVar}_n(\mathbf{Y}_n)}}.
\end{aligned}$$

2.3 dCovICA

Matteson and Tsay (2017) introduced dCovICA, an ICA method that uses distance covariance to measure dependence between sets of potential sources. The ICA model assumes that the sources $\mathbf{S} = \mathbf{A}^{-1}\mathbf{X}$ are mutually independent at the population level. The goal is to find an unmixing matrix that minimizes the empirical dependence between the unmixed components. In order to establish this mutual independence, Jin and Matteson (2018) showed that it suffices to ensure $d-1$ pairwise independencies. Their result states that the variables of \mathbf{S} are mutually independent if and only if

$$\mathbf{S}_1 \perp\!\!\!\perp \mathbf{S}_{1+}, \mathbf{S}_2 \perp\!\!\!\perp \mathbf{S}_{2+}, \dots, \mathbf{S}_{d-1} \perp\!\!\!\perp \mathbf{S}_d,$$

where $k_+ := \{l : k < l \leq d\}$.

The dCovICA method exploits this property by constructing its objective function as the sum of the empirical dependence dCov between each of these $d-1$ pairs of a random variable and a random vector. More precisely, dCovICA starts by whitening the observed data \mathbf{X}_n using

$$\mathbf{Z}_n = \mathbf{X}_n \widehat{\boldsymbol{\Sigma}}_n^{-1/2} \tag{2}$$

where $\widehat{\boldsymbol{\Sigma}}_n$ is the empirical covariance matrix. Then the separating matrix \mathbf{U} is estimated by the optimization

$$\widehat{\mathbf{U}} := \arg \min_{\mathbf{U}} \sum_{k=1}^{d-1} \text{dCov}_n(\mathbf{S}_{n,k}(\mathbf{U}), \mathbf{S}_{n,k+}(\mathbf{U})). \tag{3}$$

Here $\mathbf{S}_{n,k}(\mathbf{U})$ denotes the k -th column of $\mathbf{S}_n(\mathbf{U}) := \mathbf{Z}_n \mathbf{U}^T$, and $\mathbf{S}_{n,k_+}(\mathbf{U})$ denotes the submatrix of $\mathbf{S}_n(\mathbf{U})$ obtained by selecting the columns in $k_+ = \{l : k < l \leq d\}$.

In the population setting we have the underlying model $\mathbf{Z} = \mathbf{U}_0^T \mathbf{S}$, and replacing \mathbf{U} by \mathbf{U}_0 in the right hand side of 3 would zero each term $d\text{Cov}(\mathbf{S}_k(\mathbf{U}_0), \mathbf{S}_{k_+}(\mathbf{U}_0))$. Then the objective would become zero, and therefore attain its minimal value.

3 Robust independent component analysis

In this section we introduce our proposal for robust independent component analysis. Our approach is inspired by dCovICA, but we will introduce robustness by using a robust objective function and making some other modifications.

3.1 Robust distance correlation

The distance covariance and correlation are often credited with inherent robustness properties. Such properties were formally investigated by Leyder et al. (2024a) in the setting of measuring dependence between univariate random variables X and Y , with rather nuanced conclusions. It turned out that while distance correlation exhibits some robustness in the sense of a bounded influence function, it lacks strong robustness due to its breakdown value of 0 and the fact that its influence function does not go to zero for far outliers. To mitigate its sensitivity to outliers, its robustness was enhanced by a data transformation. The univariate datasets are first standardized to have a median of 0 and a median absolute deviation of 1. The data is then transformed using the new *biloop transform*, and finally the distance correlation is computed on the transformed data. The biloop transform is given by $\psi_\infty : \mathbb{R} \rightarrow \mathbb{R}^2 : x \mapsto (u(x), v(x))$ with

$$u(x) = \begin{cases} c(1 + \cos(2\pi \tanh(x/c) + \pi)) & \text{if } x \geq 0 \\ -c(1 + \cos(2\pi \tanh(x/c) - \pi)) & \text{if } x < 0 \end{cases}$$

$$v(x) = \sin(2\pi \tanh(x/c))$$

where $c > 0$ is a tuning constant which is set to $c = 4$ by default. Figure 1 illustrates this transformation. The innovative feature of ψ_∞ is its two-dimensional image, allowing it to go to zero for far outliers, called the *redescending property*, without crossing itself. This makes it possible for this transformation to be simultaneously one-to-one, continuous, and redescending. It needs to be one-to-one to preserve the independence property, meaning that on the population level, the

biloop distance correlation is zero if and only if the input variables are independent. Due to the redescending nature of the biloop transform, the biloop distance correlation is substantially more robust than the classical distance correlation, or the distance correlation applied to ranks.

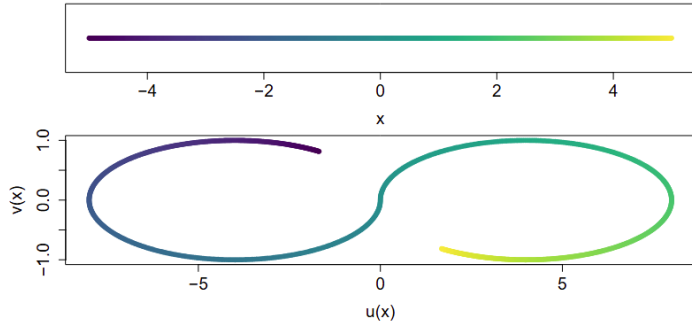


Figure 1: Illustration of the biloop transformation.

The biloop transformation was introduced for measuring dependence between two univariate random variables. In order to obtain a robust dependence measure between multivariate random variables, one could apply the biloop transform to each coordinate of the vectors separately, and then compute the distance correlation between these transformed vectors. This is a viable approach, which transforms a p -dimensional vector (with $p \leq d$) such that the transformation is one-to-one, continuous, and redescending. But the image of the vector is now in $2p$ -dimensional space, which makes the computation of subsequent distance correlations more computationally intensive.

This poses an interesting question. Can we transform a p -dimensional vector such that the transformation is bounded, one-to-one, continuous, and redescending, but with the dimension of its image lower than $2p$? The answer turns out to be positive, with a transformation to $(p+1)$ -dimensional space that achieves the three desired properties. The proposed transformation we call the *bowl transform*, defined as $\psi : \mathbb{R}^p \rightarrow \mathbb{R}^{p+1} : \mathbf{x} \mapsto (v_1(\mathbf{x}), v_2(\mathbf{x}))$ in which

$$\begin{aligned} u(\mathbf{x}) : \mathbb{R}^p &\rightarrow \mathbb{R}^1 : \mathbf{x} \mapsto \tanh\left(\frac{\|\mathbf{x}\|}{q}\right) \\ v_1(\mathbf{x}) : \mathbb{R}^p &\rightarrow \mathbb{R}^p : \mathbf{x} \mapsto 10 u(\mathbf{x})^2 (1 - u(\mathbf{x}))^2 \mathbf{x} \\ v_2(\mathbf{x}) : \mathbb{R}^p &\rightarrow \mathbb{R}^1 : \mathbf{x} \mapsto 10 u(\mathbf{x})^6 (1 - u(\mathbf{x}))^2 \end{aligned} \tag{4}$$

where $\|\mathbf{x}\|$ is the Euclidean norm of \mathbf{x} and $q = \sqrt{\chi_{0.9975, p}^2}$ is a scaling constant. Note that $v_1(\mathbf{x})$ is bounded because $(1 - u(\mathbf{x})) \rightarrow 0$ for large \mathbf{x} . The transformation is illustrated in Figure 2 for $p = 1$ and in Figure 3 for $p = 2$. We see that the image of the transformation for $p = 2$ is a rotated version of that for $p = 1$ around the z -axis. This would not have been possible with the biloop transform, because rotating it would have broken the continuity.

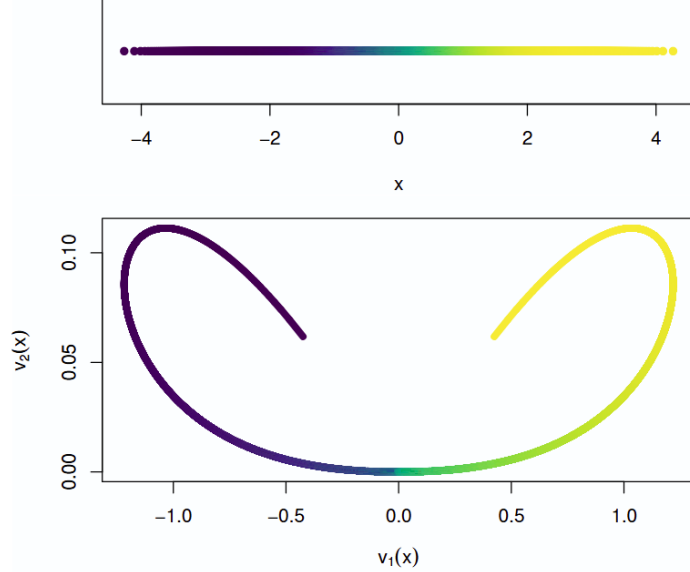


Figure 2: Illustration of the bowl transform $\psi(\mathbf{x}) = (v_1(\mathbf{x}), v_2(\mathbf{x}))$ for $p = 1$.

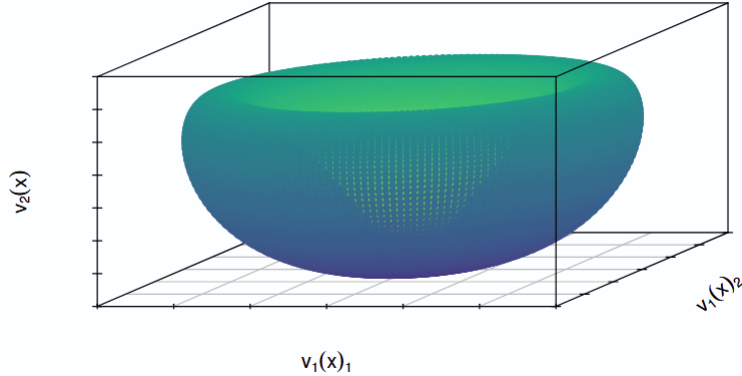


Figure 3: Illustration of the bowl transform $\psi(\mathbf{x}) = (v_1(\mathbf{x}), v_2(\mathbf{x}))$ for $p = 2$.

Computing the distance correlation of random vectors \mathbf{X} and \mathbf{Y} transformed by (4) yields the more robust dependence measure

$$\text{dCor}(\psi(\mathbf{X}), \psi(\mathbf{Y})). \quad (5)$$

It still holds that (5) is zero if and only if \mathbf{X} and \mathbf{Y} are independent, and the dimensions of \mathbf{X} and \mathbf{Y} only get increased by 1.

3.2 RICA

In order to perform robust independent component analysis, we start by whitening the data. Classical ICA and dCovICA whiten the data by (2) which employs the empirical covariance matrix $\widehat{\Sigma}_n$.

From a robustness perspective this is not ideal, as the empirical covariance matrix is highly sensitive to outliers. Its breakdown value is zero, meaning that even a single outlier can render the estimate useless. Therefore it is essential to perform whitening by a robust covariance estimator before conducting the next ICA steps, as noted by Learned-Miller and Fisher (2003), Chen et al. (2013), and Nordhausen and Oja (2018). For this whitening step we employ the Minimum Covariance Determinant (MCD) estimator of Rousseeuw (1984) computed by the algorithm of Rousseeuw and Van Driessen (1999). The MCD has excellent robustness properties, due to its bounded influence function and its breakdown value of 25% when using the default settings. This process yields the robustly whitened data

$$\mathbf{Z}_n = \mathbf{X}_n \widehat{\boldsymbol{\Sigma}}_{\text{MCD}}^{-1/2}. \quad (6)$$

After the data has been whitened, we need to estimate an orthogonal separating matrix. The goal is to find an orthogonal matrix \mathbf{U} that minimizes the empirical dependence between the components of $\mathbf{S}_n(\mathbf{U}) = \mathbf{Z}_n \mathbf{U}^T$. For this purpose the dCovICA method employs the objective function (3) based on the classical dCov measure. We modify this objective function in two ways. First, we replace the distance covariance dCov by the distance correlation dCor, which is invariant to scale differences. And secondly, we apply dCor to the data after subjecting it to the bowl transform. We therefore minimize

$$\widehat{\mathbf{U}} = \arg \min_{\mathbf{U}} \sum_{k=1}^{d-1} \text{dCor}_n(\psi(\mathbf{S}_{n,k}(\mathbf{U})), \psi(\mathbf{S}_{n,k_+}(\mathbf{U}))), \quad (7)$$

where again $\mathbf{S}_{n,k}(\mathbf{U})$ denotes the k -th column of $\mathbf{S}_n(\mathbf{U})$, and $\mathbf{S}_{n,k_+}(\mathbf{U})$ denotes the submatrix of $\mathbf{S}_n(\mathbf{U})$ consisting of the columns in $k_+ = \{l : k < l \leq d\}$.

Combining the estimated separation matrix $\widehat{\mathbf{U}}$ from (7) with the whitening matrix yields the RICA estimate of the unmixing matrix given by

$$\widehat{\mathbf{A}}^{-1} = \widehat{\boldsymbol{\Sigma}}_{\text{MCD}}^{-1/2} \widehat{\mathbf{U}}. \quad (8)$$

3.3 Optimization

Finding the optimum of the objective function in (7) is not an easy task. Following Matteson and Tsay (2017) we start by parametrizing the estimand \mathbf{U} as a product of $d(d - 1)/2$ special matrices. Because \mathbf{U} is an orthogonal matrix, there exists a doubly-indexed set of $d(d - 1)/2$ angles $\boldsymbol{\theta} \in \Theta = \{\theta_{i,j} : 1 \leq i < j \leq d : 0 \leq \theta_{1,j} < 2\pi, 0 \leq \theta_{i,j} < \pi \text{ for } i \neq 1\}$ such that \mathbf{U} can be written as

$$\mathbf{U}(\boldsymbol{\theta}) = \mathbf{Q}^{d-1} \cdot \mathbf{Q}^{d-2} \cdot \dots \cdot \mathbf{Q}^1, \quad (9)$$

where

$$\mathbf{Q}^k = \mathbf{Q}_{k,d}(\theta_{k,d}) \cdot \mathbf{Q}_{k,d-1}(\theta_{k,d-1}) \cdot \dots \cdot \mathbf{Q}_{k,k+1}(\theta_{k,k+1}).$$

In the above expressions, $\mathbf{Q}_{i,j}(\theta_{i,j})$ denotes a Givens rotation matrix. It is derived from the identity matrix \mathbf{I}_d where the entries at (i,i) and (j,j) are replaced by $\cos(\theta_{i,j})$, the (i,j) entry by $\sin(\theta_{i,j})$, and the (j,i) entry by $-\sin(\theta_{i,j})$. It is worth noting that there exists a unique $\boldsymbol{\theta}$ in Θ yielding $\mathbf{U}(\boldsymbol{\theta})$ whenever all entries on the diagonal of \mathbf{U} are positive or all entries of \mathbf{U} are nonzero.

We can thus rewrite the objective function in terms of $\boldsymbol{\theta}$, where we are now optimizing over a set of $d(d-1)/2$ angles:

$$\hat{\boldsymbol{\theta}} = \arg \min_{\boldsymbol{\theta} \in \Theta} \sum_{k=1}^{d-1} \text{dCor}_n(\psi(\mathbf{S}_{n,k}(\mathbf{U}(\boldsymbol{\theta}))), \psi(\mathbf{S}_{n,k+1}(\mathbf{U}(\boldsymbol{\theta})))) . \quad (10)$$

The decomposition (9) implies that the k^{th} row of $\mathbf{U}(\boldsymbol{\theta})$ depends only on the k^{th} row of a product with fewer factors, namely $\mathbf{Q}^k \cdot \mathbf{Q}^{k-1} \cdot \dots \cdot \mathbf{Q}^1$. Therefore the k^{th} independent component $\mathbf{S}_k(\boldsymbol{\theta})$ only depends on the angles $\{\theta_{i,j} : i < j \leq d \text{ for } i = 1, 2, \dots, k\}$, which allows us to estimate the angles sequentially. First, estimate the $d-1$ angles $\theta_{1,j}$ yielding the estimate $\mathbf{S}_1(\boldsymbol{\theta})$. Next, estimate the $d-2$ angles for recovering $\mathbf{S}_2(\boldsymbol{\theta})$ in the subspace orthogonal to the one spanned by $\mathbf{S}_1(\boldsymbol{\theta})$. We continue this process, each time working in the lower-dimensional subspace orthogonal to the space spanned by the previously estimated components, and estimate the angles of the next component. Compared to the joint estimation of all the angles in (10), the sequential approach is computationally cheaper and faster. In principle this could come at the cost of a lower accuracy. However, in our experiments and using the optimization procedure and refinement steps described below, we found that this was not the case. Therefore RICA will use the sequential approach for all results in this paper.

The sequential estimation in RICA gives rise to $d-1$ optimization problems, each time estimating $d-k$ angles $\theta_{k,k+1}, \dots, \theta_{k,d}$. For these optimizations we employ the derivative-free solver COBYQA (Constrained Optimization BY Quadratic Approximations) of Ragonneau (2022). This choice is motivated by the challenges of our setting, the computation of the bowl transform and the $\mathcal{O}(n^2)$ computational cost per evaluation of the distance correlation, which together make it challenging to derive and numerically compute exact gradients. As a derivative-free, trust-region, sequential quadratic programming method, COBYQA is designed for such scenarios. It operates by iteratively building and refining quadratic models of the objective and constraint functions using the derivative-free symmetric Broyden update, effectively modeling our complex landscape. For angle optimization it is important that COBYQA always respects region constraints, ensuring

that all iterated angles remain within the specified ranges. The combination of COBYQA’s efficient derivative-free optimization and its strict adherence to essential bound constraints makes it a well-suited choice for our optimization task.

Finally, we refine our optimization by incorporating a technique from the RADICAL method of Learned-Miller and Fisher (2003). They also optimize by using $d(d-1)/2$ two-dimensional rotations to estimate the orthogonal separating matrix \mathbf{U} , a process they refer to as a “sweep”. However, after obtaining a matrix of sources \mathbf{S}_n through this process, they iteratively apply such sweeps multiple times until the change in the matrix $\hat{\mathbf{U}}$ falls below some threshold. We have opted to perform multiple sweeps also. In particular, after optimizing the $d(d-1)/2$ angles in $\boldsymbol{\theta}$, we permute the columns of the resulting $\mathbf{S}_n(\boldsymbol{\theta})$ and repeat the optimization on it, referring to this as a sweep. Empirically, we found that performing $d+1$ sweeps substantially improved the accuracy, in line with the findings in the RADICAL paper. On the other hand, this also increased the runtime. The use of sweeps thus involves a trade-off between accuracy and computational efficiency. Therefore, we will compare RICA with the version without sweeps in the simulations in Section 5.

4 Theoretical analysis

In this section we establish almost sure convergence and root- n consistency of the RICA estimator. There are two key differences between these results and those previously obtained by Matteson and Tsay (2017). The first is that we use the distance correlation rather than the distance covariance. The second is that we have introduced the bowl transform ψ which is applied to the data before measuring dependence. As the bowl transform is bounded, the first and second moments of the transformed data always exist. Therefore, we do not require any moment assumptions on the original data distribution. Moreover, we will use the fact that the bowl transform is Lipschitz continuous, as it is continuously differentiable with bounded derivative.

First we need the population counterpart of (10). We define the population parameter θ_0 as

$$\boldsymbol{\theta}_0 = \arg \min_{\boldsymbol{\theta} \in \Theta} \sum_{k=1}^{d-1} \text{dCor}(\psi(\mathbf{S}_k(\mathbf{U}(\boldsymbol{\theta}))), \psi(\mathbf{S}_{k+}(\mathbf{U}(\boldsymbol{\theta})))) . \quad (11)$$

The following proposition states the almost sure convergence of $\hat{\boldsymbol{\theta}}_n$ to $\boldsymbol{\theta}_0$. We consider a large compact subset $\overline{\Theta}$ of the parameter space Θ .

Proposition 1. *If there exists a unique minimum $\boldsymbol{\theta}_0$ of (11) over $\overline{\Theta}$, and $\boldsymbol{\theta}_0$ is the only $\boldsymbol{\theta}$ in Θ yielding $\mathbf{U}(\boldsymbol{\theta}) = \mathbf{U}(\boldsymbol{\theta}_0)$, then we have almost sure convergence for its empirical counterpart in (10), that is $\hat{\boldsymbol{\theta}}_n \xrightarrow{a.s.} \boldsymbol{\theta}_0$.*

Further details on the required lemmas, their proofs, and the proof of the proposition are provided in the Supplementary Material. Next, we present the result on root- n consistency, with its proof also available in the Supplementary Material.

Proposition 2. *Under the same assumptions as Proposition 1 we have root- n consistency, that is, $\|\hat{\boldsymbol{\theta}}_n - \boldsymbol{\theta}_0\| = O_P(n^{-1/2})$.*

We conclude that if the ICA model $\mathbf{S} = \mathbf{U}(\boldsymbol{\theta}_0)\mathbf{Z}$ holds, the estimator in 7 is strongly consistent and converges at the usual parametric rate of $1/\sqrt{n}$.

5 Simulation results

In this section we evaluate RICA by an extensive simulation study. We compare its performance against various state-of-the-art ICA techniques. We will examine different contamination scenarios, sample from a range of distributions, and consider different dimensions.

5.1 Setting

Simulations evaluating the performance of ICA methods typically rely on a standardized set of benchmark distributions, as in Bach and Jordan (2002), Learned-Miller and Fisher (2003), and Matteson and Tsay (2017). Following this convention, we base our analysis on the 18 distributions outlined in Hastie et al. (2009). The corresponding distributions, depicted in Figure 4, include Student- t distributions, symmetric and asymmetric Gaussian mixtures, and exponential mixtures.

We consider 3 main settings for sampling the data, depending on the contamination added. The first setting comprises uncontaminated data. For this, the columns of the $n \times d$ matrix of data sources \mathbf{S}_n are sampled from the 18 distributions. For the contaminated settings we consider two scenarios from Brys et al. (2005), called multiplicative and clustered contamination.

For clustered contamination we begin with an uncontaminated \mathbf{S}_n as before, but then replace 10% of the rows by observations sampled from $\mathcal{N}(15, 1)$. For multiplicative contamination, we instead replace 10% of the rows as follows. For each selected row, we generate a vector of size d with values sampled from the uniform distribution on $[0, 1]$, ensuring that its sum is greater than 1. Then this vector is multiplied by d and by either the minimum or maximum value of the source in each column, with the choice between the two made randomly, before replacing the row with it. In this way outliers are positioned on either side of the bulk of the data points.

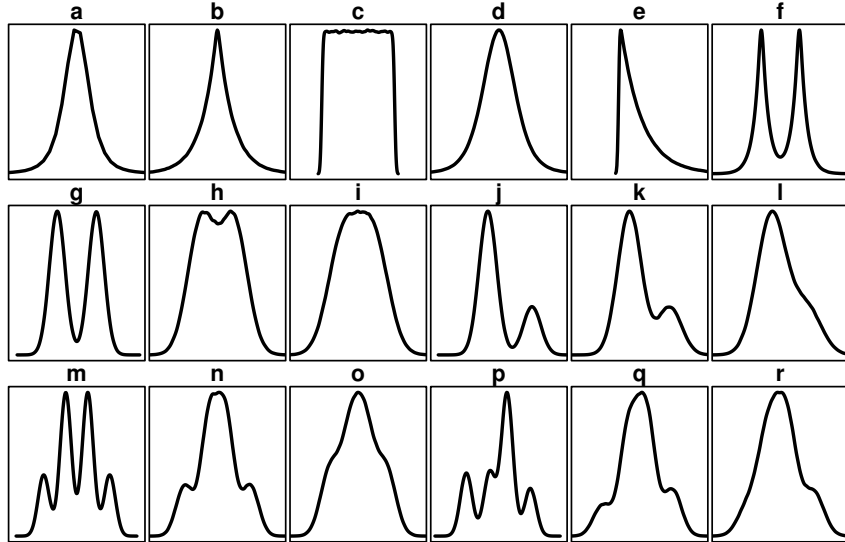


Figure 4: The 18 source distributions used in the simulations.

After the independent sources \mathbf{S}_n are generated, we generate random $d \times d$ mixing matrices A that are well-conditioned in the sense that their condition number is between 1 and 2. We then compute the mixed data $\mathbf{X}_n = \mathbf{S}_n \mathbf{A}^T$ that is the input of the ICA methods.

We sample data in this manner for three different dimensions d as follows:

- For $d = 2$ we generate $n = 1000$ observations per dataset and perform 1000 replications;
- For $d = 4$ we generate $n = 1000$ observations per dataset and perform 100 replications;
- For $d = 6$ we generate $n = 2000$ observations per dataset and perform 100 replications.

We repeat this process for each of the 18 distributions and for each of the three contamination settings.

We compare RICA to the FastICA, JADE, infomax, and dCovICA methods, that start with their classical whitening step. We also include the robust RADICAL method, that we run with its built-in robust whitening step.

For FastICA we used its implementation in the Python library *scikit-learn* (Pedregosa et al., 2011), with the exponential function as its non-linearity because this has the best robustness properties (Hyvärinen, 1999). Infomax and JADE were obtained from the R package *ica* (Helwig, 2022), while RADICAL was sourced from the R package *rmgarch* (Galanos, 2022). For dCovICA and RICA we wrote our own Python implementation, using *scipy* (Virtanen et al., 2020) for the optimization. For the MCD whitening we used *robpy* (Leyder et al., 2024b).

To examine the performance of the different ICA methods we require an evaluation metric.

Direct comparison of the estimated mixing matrices \mathbf{A} is not possible due to inherent indeterminacies in scale, sign, and permutation, as discussed in Section 2.1. To bypass this, we use the Amari error as a measure of inaccuracy (Amari et al., 1995):

$$\frac{\sum_{i=1}^d \sum_{j=1}^d \left(\frac{|\mathbf{P}_{ij}|}{\max_k |\mathbf{P}_{ik}|} - 1 \right) + \sum_{j=1}^d \sum_{i=1}^d \left(\frac{|\mathbf{P}_{ij}|}{\max_k |\mathbf{P}_{kj}|} - 1 \right)}{2d(d-1)}.$$

Here $\mathbf{P} = \mathbf{UW}\mathbf{A}$ is the product of the estimated unmixing matrix \mathbf{UW} obtained from the ICA algorithm, and the true mixing matrix \mathbf{A} . The Amari measure is invariant to ICA indeterminacies and ranges from 0 to 1, where 0 indicates the best possible performance and 1 the worst.

5.2 Results

The simulation results are organized by the type of contamination: first those for uncontaminated data are shown, then with clustered contamination, and finally with multiplicative contamination.

The Amari error is averaged over the replications per setting, and the average Amari error of a method is displayed in function of the distribution type on the horizontal axis, as in Figure 5. This is common practice in the ICA literature (Hastie et al., 2009). This visualization makes it easier to compare ICA methods than by looking at large tables. But for completeness, we also provide the numerical results in tabular form in the Supplementary Material.

To enhance the readability and to highlight the performance of RICA we have ordered the distributions on the horizontal axis of each plot according to the results obtained by the default version of RICA, which is the one with optimization sweeps.

5.2.1 Uncontaminated data

Figure 5 shows the simulation results on uncontaminated data, with one plot per dimension. It also includes a small table listing the average Amari error over all 18 distributions, with the lowest error per column in boldface.

From the results we conclude that even when there is no contamination, RICA performed very well. While other methods attain both high and low errors, reflecting sensitivity to the underlying distribution type, RICA exhibits a more stable performance with less variation. In dimensions 4 and 6 it was the best-performing method based on the average error over all distributions.

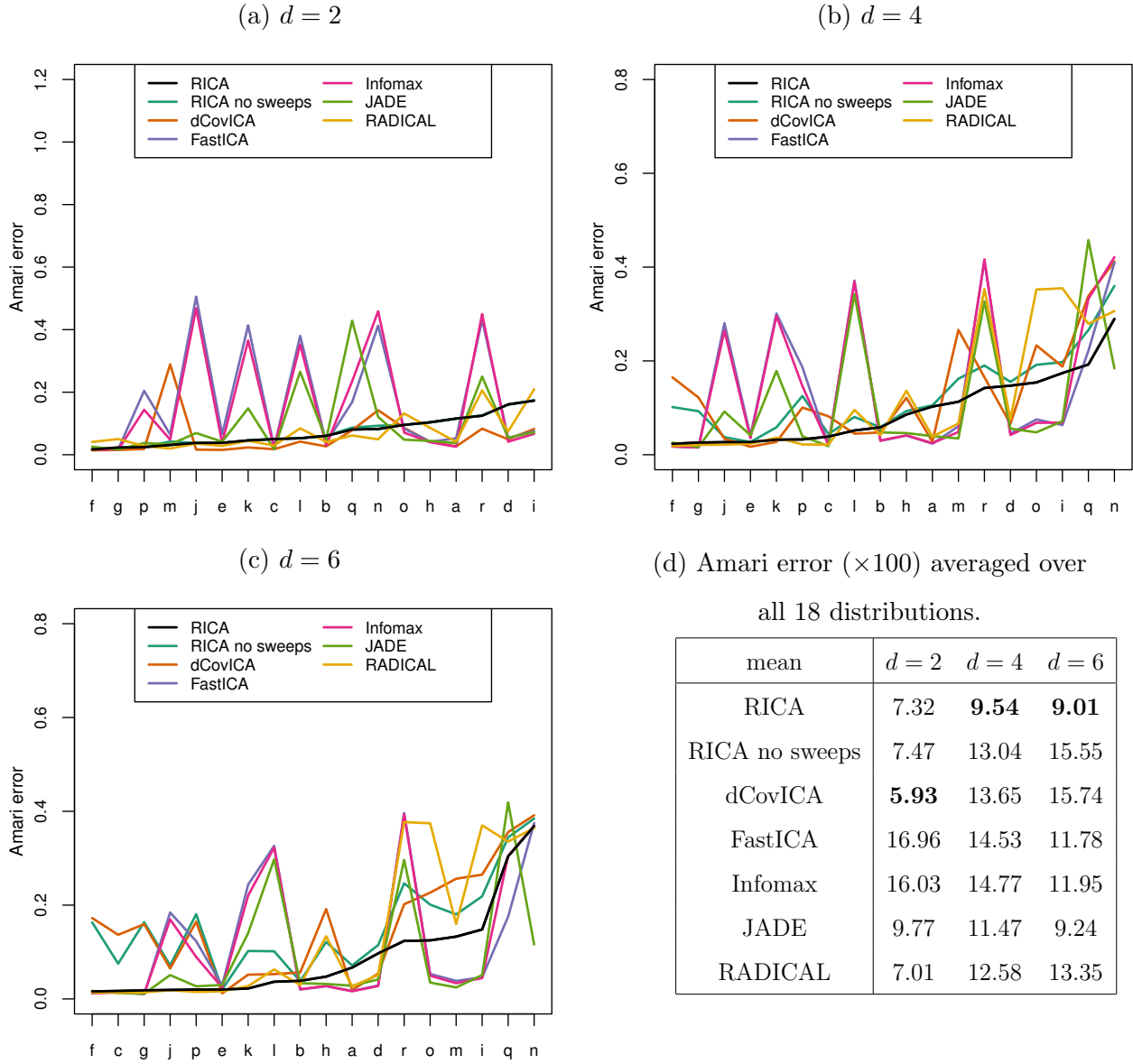


Figure 5: Simulation results for uncontaminated data.

5.2.2 Clustered contamination

When 10% of clustered contamination was introduced into the data, Figure 6 indicates that most ICA methods lost their competitiveness, while RICA remained the only method maintaining low Amari errors. It is worth noting that a random non-singular matrix will typically yield an Amari error around 0.4 (Nordhausen et al., 2011b), suggesting that for such clustered contamination data, most ICA methods performed no better than making a random guess.

We also observe that the beneficial effect of performing optimization sweeps on the accuracy remains as strong as it was for uncontaminated data, particularly as the dimension increased. This

is why our default version of RICA is with the sweeps.

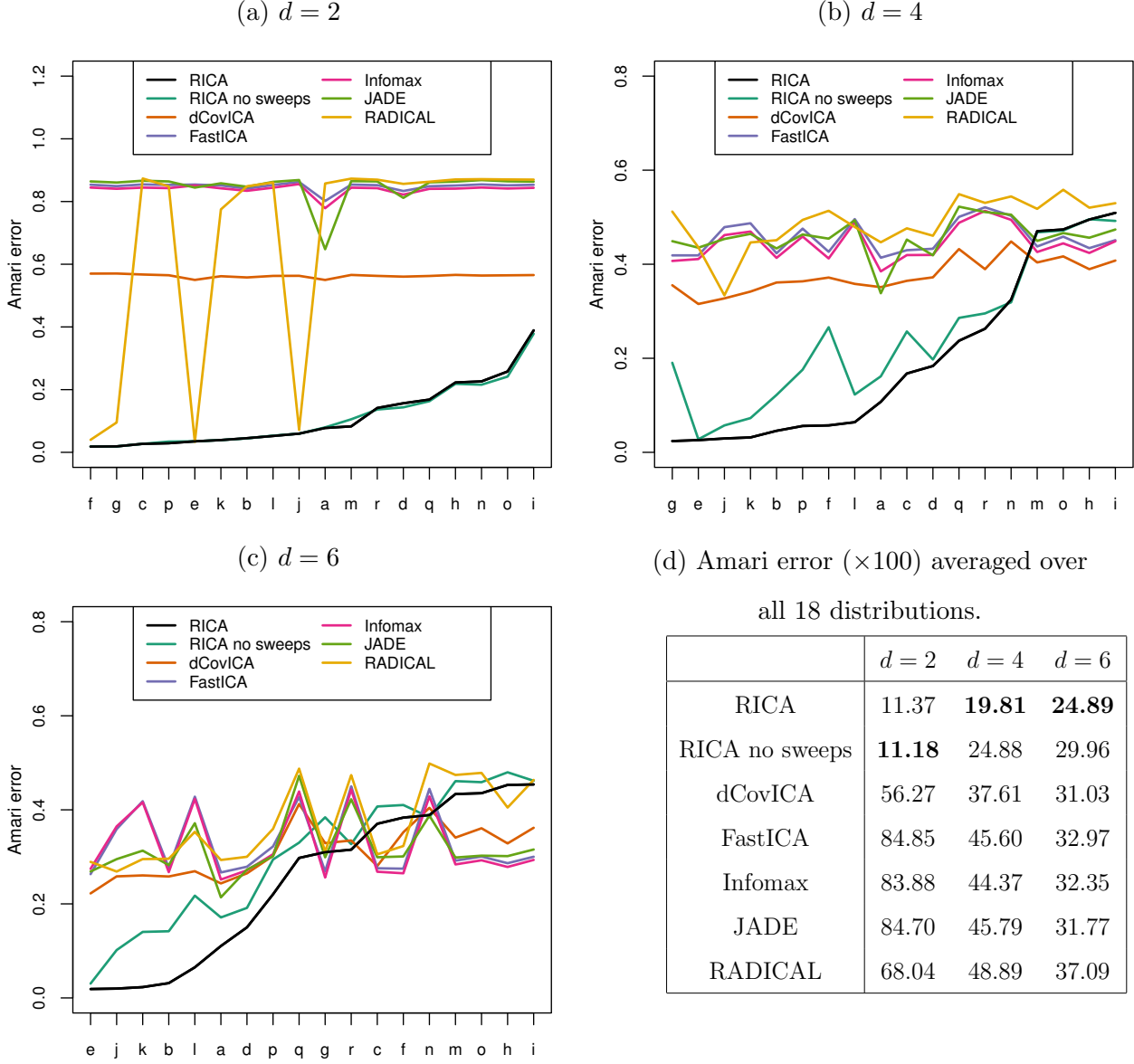


Figure 6: Simulation results for clustered contamination.

5.2.3 Multiplicative contamination

Lastly, the results for multiplicative contamination are shown in Figure 7. While RICA is again the most effective method in the presence of outliers, RADICAL does outperform the remaining methods. This is not surprising, as insensitivity to outliers was one of its design goals. However, its effectiveness depends on the distribution of the sources, as it worked very well in some settings and did worse than a random guess in others. We also see that dCovICA performs well at certain

distributions. Indeed, in Section 3.1 we saw that the standard dCov has some robustness properties, but perhaps not enough.

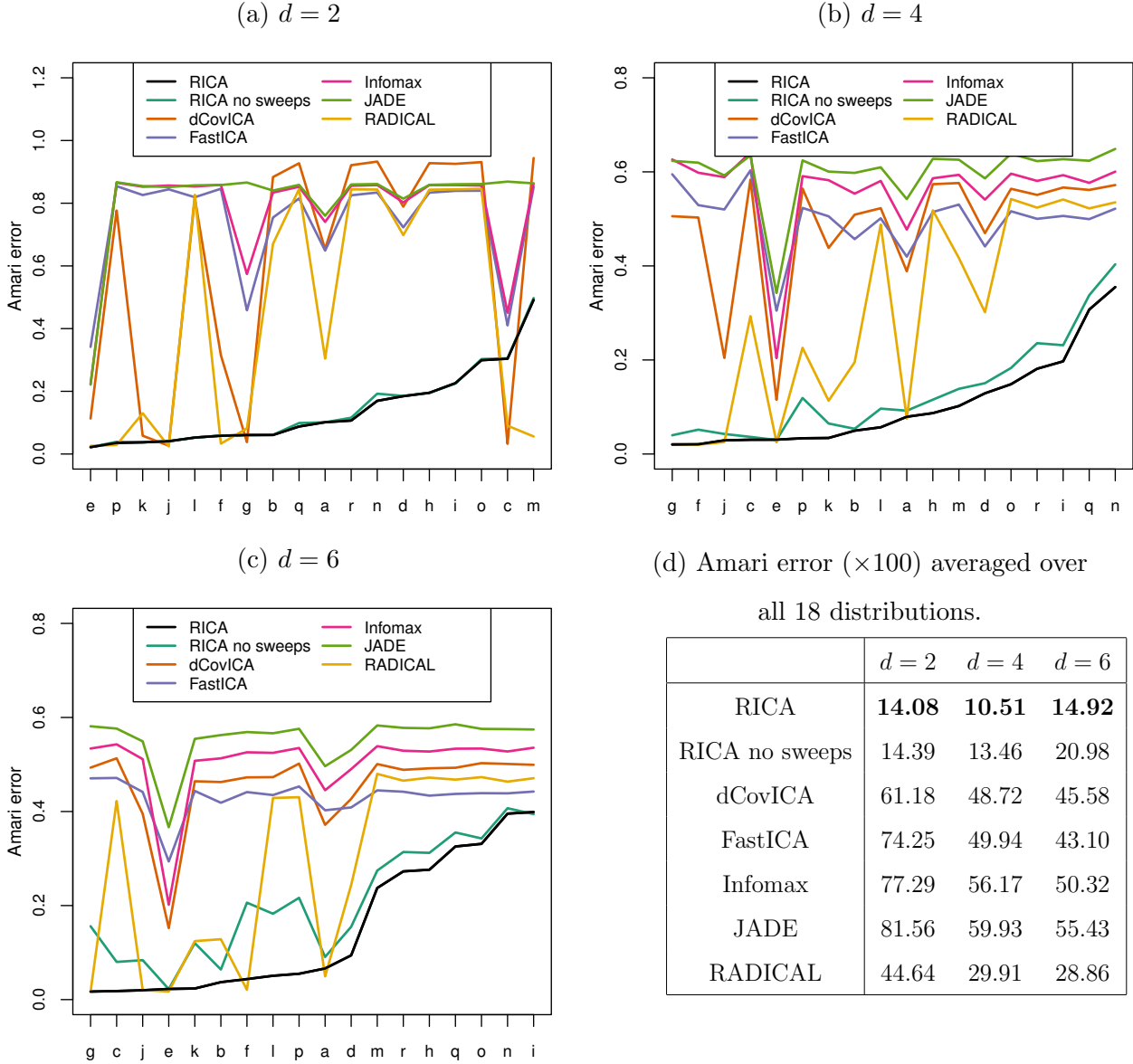


Figure 7: Simulation results for multiplicative contamination.

5.3 Increasing contamination

Following Bach and Jordan (2002) and Learned-Miller and Fisher (2003), we conducted an experiment to investigate the effect of gradually introducing more and more outliers. Starting from outlier-free datasets, we progressively increase the proportion of outliers up to 20%.

We start with bivariate datasets of 1000 observations, where each source was sampled uniformly at random from the 18 previously defined distributions. We then introduced outliers step by step, each time drawing one more data point and replacing a randomly selected coordinate of that point by either +5 or -5, with equal probability. This is repeated until the number of outliers reaches 200, so the contamination level ranges from 0% to 20%. The experiment was replicated 1000 times to ensure reliable results.

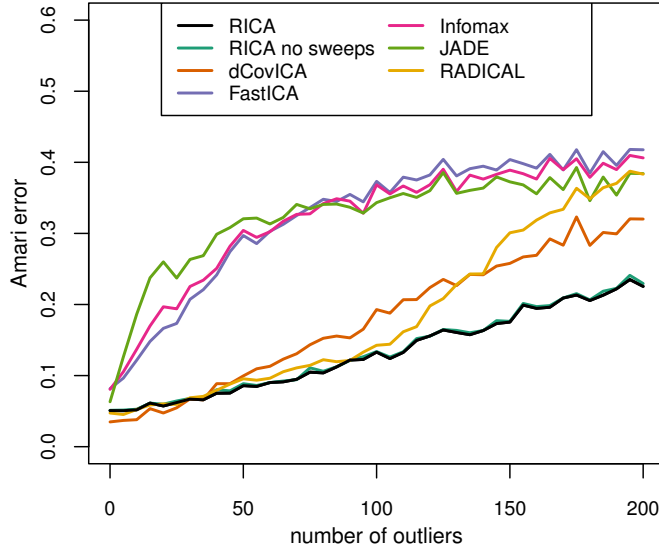


Figure 8: Effect of increasing number of outliers for $d = 2$.

Figure 8 plots the average Amari error in function of the number of outliers. For all methods the error goes up with the amount of contamination, with RICA being the least affected. RADICAL also achieves good results initially, but for more than 10% of outliers its performance deteriorates. The dCovICA method performs well up to 5% of outliers, after which it becomes less effective. FastICA, infomax and JADE are affected already for a small number of outliers.

6 Real data examples

In this section, we illustrate RICA on real datasets containing outliers. For this we use image data, audio data, and periodic signals.

6.1 Image data

As a first example, we use three images from the *scikit-image* package in Python (van der Walt et al., 2014): an astronaut, grass, and a cat. The grayscale images are 128×128 . Storing the pixels in a tall column vector, this yields a 16384×3 dataset. We then introduce outliers in each image by randomly selecting 250 pixels and turning them into black pixels, which amounts to 1.5% of contamination. The images are then mixed using a random 3×3 orthogonal matrix \mathbf{A} , and we attempt to reconstruct the original ones.

In Figure 9 we see that RICA is the only method that successfully recovers the original images. In contrast, the other three methods fail to separate the sources correctly, as the cat appears in two of the reconstructed images.

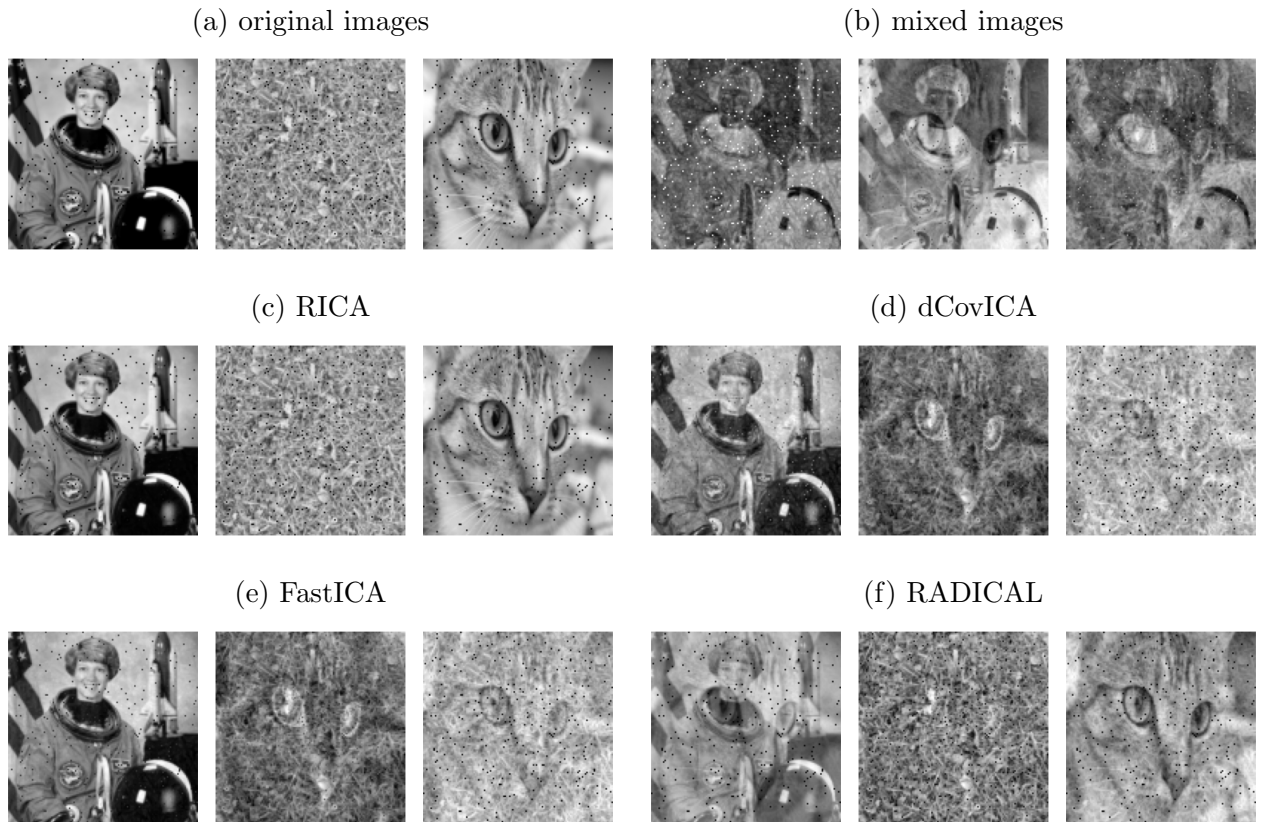


Figure 9: Mixed images example.

6.2 Cocktail party problem

Another application of ICA is to the well-known cocktail party problem, a scenario in which multiple overlapping signals, such as speech from different speakers, are recorded through multiple

microphones. The objective is to separate these mixed signals without prior knowledge about the original sources.

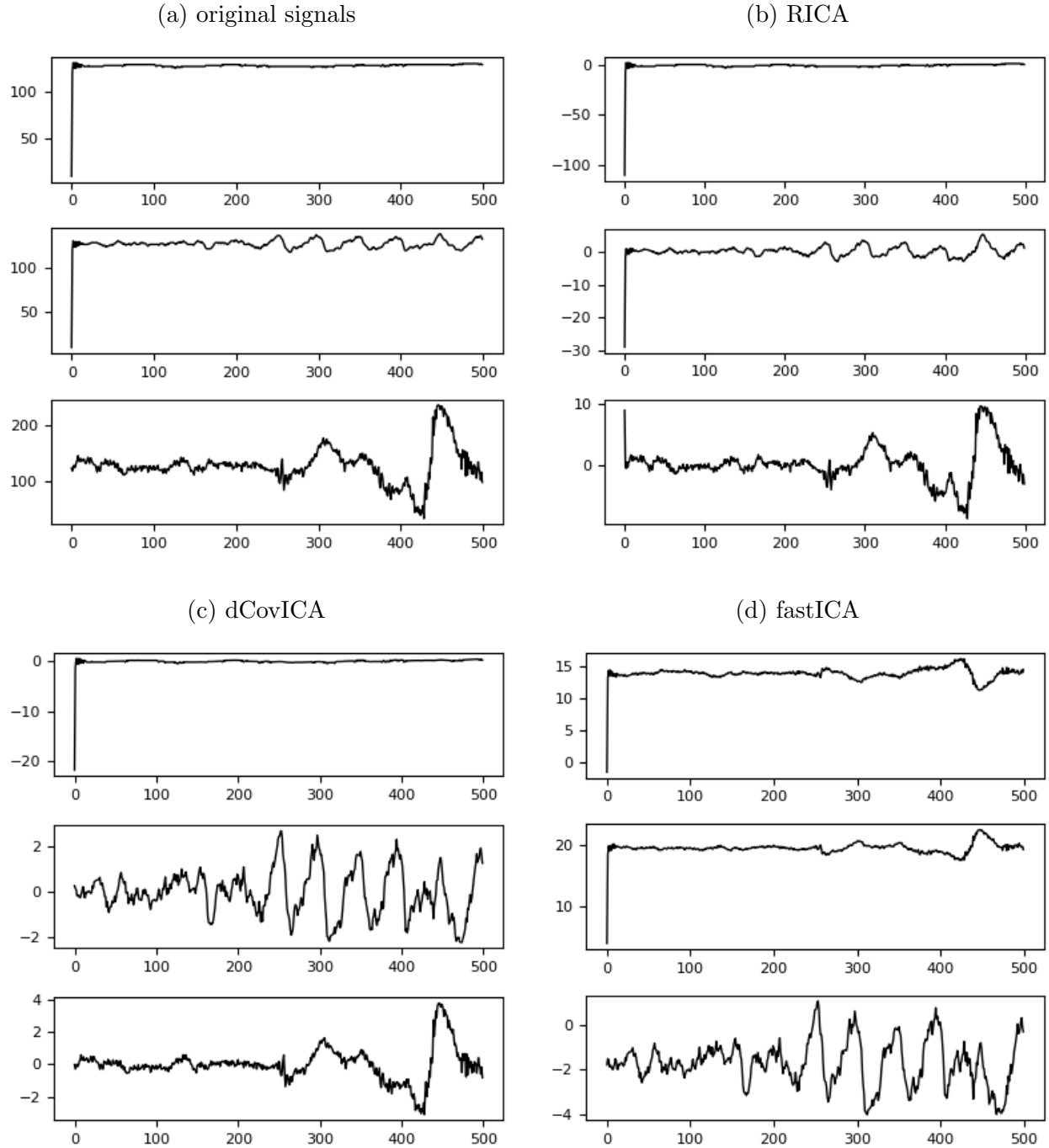


Figure 10: Cocktail party example on *JADE* data.

We first illustrate this problem on the cocktail party data from the *JADE* package (Miettinen et al., 2017) in R. We select the first 500 cases, where an artifact stands out in two of the three

sources at the start of the recording, likely due to turning on the microphones or the recorder. The artifact is clearly visible in the top two time series in the northwest panel of Figure 10. The three sources are mixed by a random 3×3 orthogonal matrix.

We then apply RICA, dCovICA, and FastICA. The results are shown in the three remaining panels of Figure 10. We see that only RICA successfully separates the signals, while both dCovICA and FastICA are significantly affected by the outlier. The corresponding Amari errors further support this: RICA achieves the lowest error (0.0875), followed by dCovICA (0.2326) and FastICA (0.4895).

After removing the outlying observation from the data set, dCovICA and FastICA perform better, with Amari errors of 0.0905 and 0.2714. The error of RICA stays about the same at 0.0992, so it was minimally affected by the outlier.

A second cocktail party dataset containing outliers is from Brys et al. (2005). This dataset consists of 5000 observations of two signals, with a loud external noise occurring in the middle. This noise affects both sources, introducing dependence between the signals.

Figure 11 shows the sources before mixing, and the unmixing results of RICA, dCovICA and FastICA. Again RICA is the only method recovering the original signals, while dCovICA and FastICA are affected by the external noise and attribute the noise to a single source. RICA attains a low Amari error (0.017), while dCovICA and FastICA obtain high errors (0.549 and 0.590).

6.3 Periodic data

Lastly we replicate the periodic signals from Brys et al. (2005). This setup involves generating three periodic sources:

$$\sin(3t), \text{sawtooth}(19t), \log(\text{rem}(t, \pi)),$$

for $t = -10\pi, -10\pi + 0.1, \dots, 10\pi$. Here `sawtooth` repeats a linear function, and `rem` is the remainder function. We then contaminate the sawtooth signal by 1.5% of outliers, represented as vertical lines in Figure 12. After mixing the data we apply RICA, dCovICA, and FastICA, yielding the remaining panels of Figure 12. Both dCovICA and FastICA struggle to recover the third signal, which becomes quite noisy and gets an upward spike near the end. RICA does reproduce the signals and attains the lowest Amari error (0.0111), followed by dCovICA (0.0742) and FastICA (0.1001).

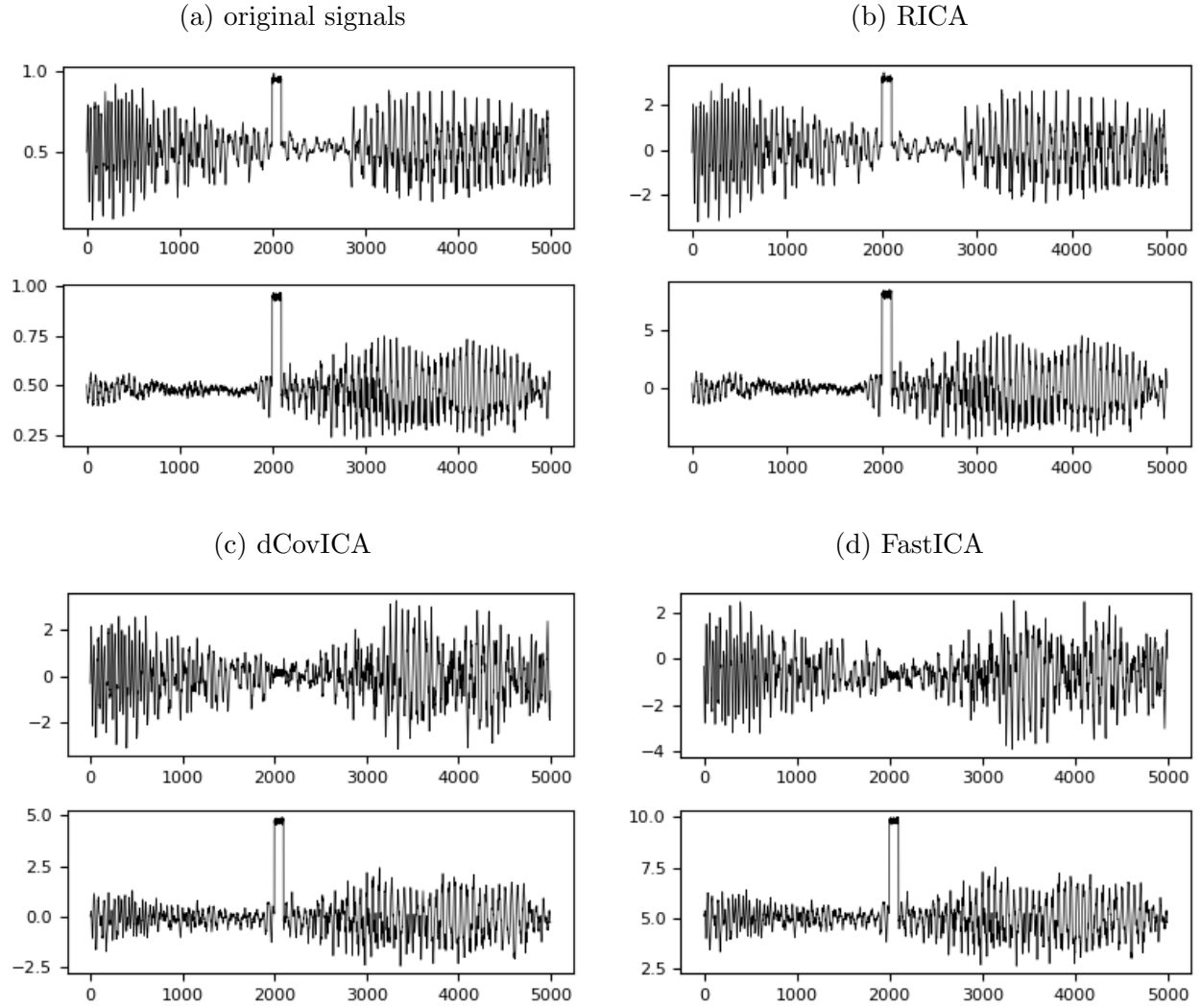


Figure 11: Cocktail party example on the Brys et al data.

7 Discussion

Independent component analysis (ICA) is a powerful tool in signal processing. Unfortunately, most popular approaches for ICA are not robust against outliers, for instance because they use higher-order statistics. In the literature several methods have been proposed that aim to be more robust, based on various principles. Some approaches involved a robust choice of contrast function, and others used preprocessing, nonparametrics, or divergences. In this paper we proposed a robust ICA method called RICA, which proceeds by estimating the separating matrix by minimizing a robust measure of dependence between vector variables.

The dependence measure used is the distance correlation (dCor) of Székely et al. (2007), whereas

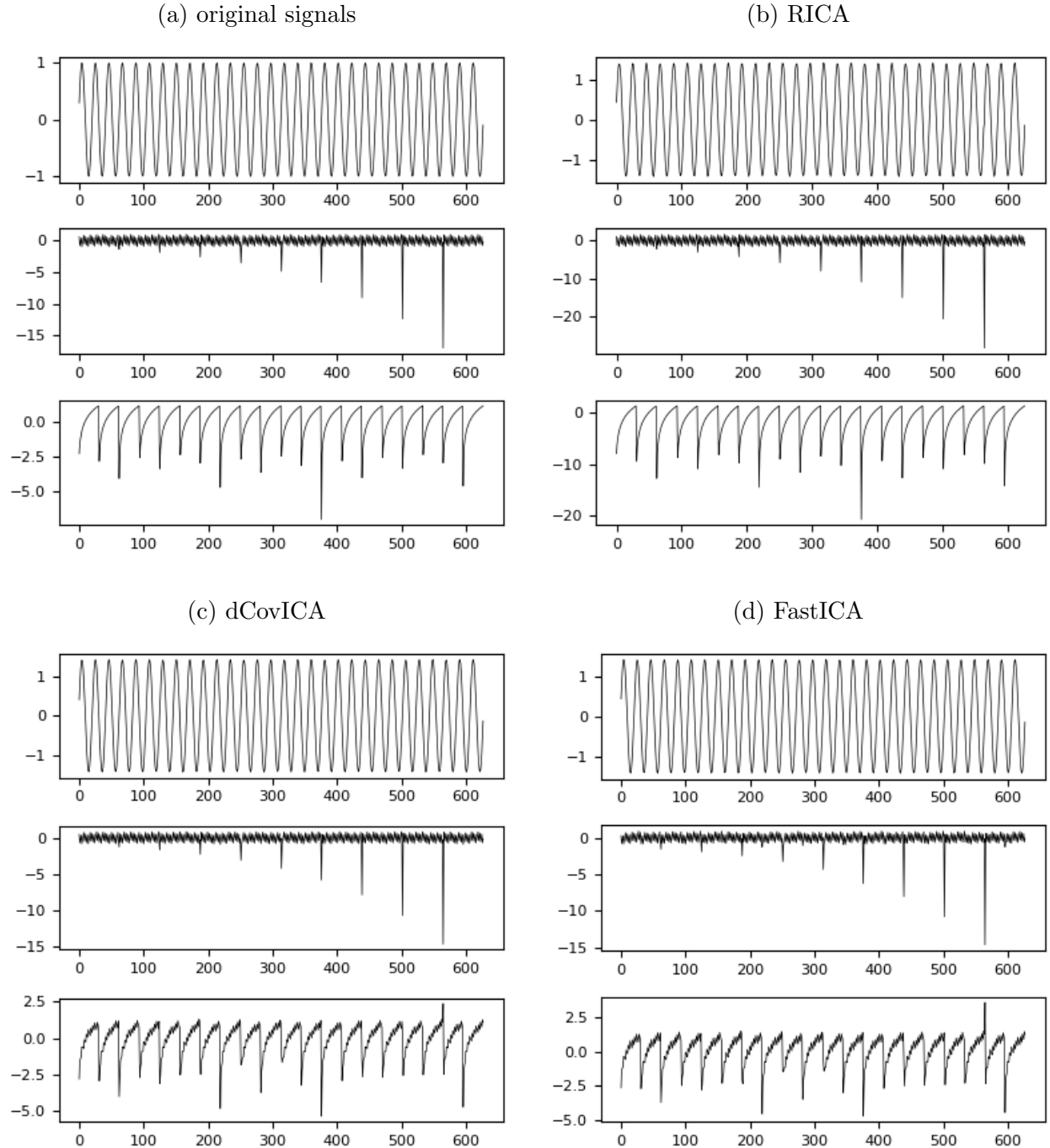


Figure 12: Periodic data example.

other authors have used the distance covariance. In order to make the distance correlation more robust we constructed a new transformation called the bowl transform, which maps p -dimensional space to a manifold in $p+1$ dimensions. This transform is bounded, one-to-one, and continuous. It is also redescending, meaning that far outliers are mapped to points close to the origin. By computing

the dCor after transforming its inputs it becomes more robust to outliers, while preserving the crucial property that a dCor of zero characterizes independence. The RICA method estimates the independent sources sequentially, by looking for the component which has the smallest dCor with the remainder projected on its orthogonal complement.

We showed that RICA is strongly consistent and has the usual parametric rate of convergence. Its robustness was investigated empirically by a simulation study, in which it outperformed its competitors most of the time and on average. RICA was illustrated in three applications, including the well-known cocktail party problem.

It is worth noting that combining robustness with measuring independence is a balancing act. Robust methods aim to reduce the effect of extreme observations. However, if the true dependence mainly comes from the tails of the distributions of the sources, a robust method may miss it. With this in mind, it is recommended to compare the results of a robust method with those of a classical method. If the outcomes are similar, all is well. If the outcomes are different, one has to study the results in order to decide whether the extreme points in question are part of the structure we want to model, or due to unwanted data contamination.

Among potential directions for future research could be extensions of RICA to blind source separation, or to estimation in the noisy ICA model described in e.g. (Voss et al., 2015).

Acknowledgment. We are grateful to Art Owen for asking the question that motivated us to construct the bowl transform.

References

- Amari, S.-I., Cichocki, A., and Yang, H. H. (1995). A new learning algorithm for blind signal separation. *Advances in Neural Information Processing Systems (NeurIPS)*, 8:757–763.
- Ans, B., Hérault, J., and Jutten, C. (1985). Architectures neuromimétiques adaptatives: Détection de primitives. *Cognitiva*, 2:593–597.
- Bach, F. R. and Jordan, M. I. (2002). Kernel independent component analysis. *Journal of Machine Learning Research*, 3:1–48.
- Bell, A. J. and Sejnowski, T. J. (1995). An information-maximization approach to blind separation and blind deconvolution. *Neural Computation*, 7(6):1129–1159.

- Bryls, G., Hubert, M., and Rousseeuw, P. (2005). A robustification of independent component analysis. *Journal of Chemometrics*, 19:364–375.
- Cardoso, J.-F. (1998). Blind signal separation: Statistical principles. *Proceedings of the IEEE*, 90(8):2009–2025.
- Cardoso, J.-F. and Souloumiac, A. (1993). Blind beamforming for non-gaussian signals. *IEE Proceedings F (Radar and Signal Processing)*, 140:362–370.
- Chen, A. and Bickel, P. J. (2005). Consistent independent component analysis and prewhitening. *IEEE Transactions on Signal Processing*, 53(10):3625–3632.
- Chen, P., Hung, H., Komori, O., Huang, S.-Y., and Eguchi, S. (2013). Robust independent component analysis via minimum γ -divergence estimation. *IEEE Journal of Selected Topics in Signal Processing*, 7(4):614–624.
- Comon, P. (1994). Independent component analysis, a new concept? *Signal Processing*, 36(3):287–314.
- Comon, P. and Jutten, C. (2010). *Handbook of Blind Source Separation: Independent Component Analysis and Applications*. Academic press.
- Galanos, A. (2022). *rmgarch: Multivariate GARCH models*. R package version 1.3-9, <https://CRAN.R-project.org/package=rmgarch>.
- Hampel, F. R., Ronchetti, E. M., Rousseeuw, P. J., and Stahel, W. A. (1986). *Robust Statistics: the Approach Based on Influence Functions*. Wiley, New York.
- Hastie, T., Tibshirani, R., and Friedman, J. (2009). *The Elements of Statistical Learning: Data Mining, Inference, and Prediction, 2nd Edition*. Springer, New York.
- Helwig, N. E. (2022). *ica: Independent Component Analysis*. R package version 1.0-3, <https://CRAN.R-project.org/package=ica>.
- Hyvärinen, A. (1999). Fast and robust fixed-point algorithms for independent component analysis. *IEEE Transactions on Neural Networks*, 10(3):626–634.
- Hyvärinen, A., Karhunen, J., and Oja, E. (2001). *Independent Component Analysis*. Wiley, New York.

- Hyvärinen, A. and Oja, E. (1997). A fast fixed-point algorithm for independent component analysis. *Neural Computation*, 9(7):1483–1492.
- Hyvärinen, A. and Oja, E. (2000). Independent component analysis: algorithms and applications. *Neural Networks*, 13(4-5):411–430.
- Jin, Z. and Matteson, D. S. (2018). Generalizing distance covariance to measure and test multivariate mutual dependence via complete and incomplete V-statistics. *Journal of Multivariate Analysis*, 168:304–322.
- Learned-Miller, E. G. and Fisher, J. W. (2003). ICA using spacings estimates of entropy. *Journal of Machine Learning Research*, 4:1271–1295.
- Lee, T.-W., Girolami, M., and Sejnowski, T. J. (1999). Independent component analysis using an extended infomax algorithm for mixed subgaussian and supergaussian sources. *Neural Computation*, 11(2):417–441.
- Leyder, S., Raymaekers, J., and Rousseeuw, P. J. (2024a). Robust Distance Correlation. *International Statistical Review*, to appear. arXiv preprint 2403.03722.
- Leyder, S., Raymaekers, J., Rousseeuw, P. J., Servotte, T., and Verdonck, T. (2024b). RobPy: a Python Package for Robust Statistical Methods. *arXiv*, preprint 2411.01954.
- Matteson, D. S. and Tsay, R. S. (2017). Independent Component Analysis via Distance Covariance. *Journal of the American Statistical Association*, 112(518):623–637.
- Miettinen, J., Nordhausen, K., and Taskinen, S. (2017). Blind source separation based on joint diagonalization in R: The packages JADE and BSSasymp. *Journal of Statistical Software*, 76:1–31.
- Miettinen, J., Taskinen, S., Nordhausen, K., and Oja, H. (2015). Fourth moments and independent component analysis. *Statistical Science*, 30(3):372–390.
- Naik, G. R. and Kumar, D. K. (2011). An overview of independent component analysis and its applications. *Informatica*, 35(1):63–81.
- Nordhausen, K., Ilmonen, P., Mandal, A., Oja, H., and Ollila, E. (2011a). Deflation-based FastICA reloaded. In *19th European Signal Processing Conference*, pages 1854–1858. IEEE.

Nordhausen, K. and Oja, H. (2018). Independent component analysis: A statistical perspective.

Wiley Interdisciplinary Reviews: Computational Statistics, 10(5).

Nordhausen, K., Ollila, E., and Oja, H. (2011b). On the performance indices of ICA and blind source separation. In *2011 IEEE 12th International Workshop on Signal Processing Advances in Wireless Communications*, pages 486–490. IEEE.

Ollila, E. (2009). The deflation-based FastICA estimator: Statistical analysis revisited. *IEEE Transactions on Signal Processing*, 58(3):1527–1541.

Pedregosa, F., Varoquaux, G., Gramfort, A., Michel, V., Thirion, B., Grisel, O., Blondel, M., Prettenhofer, P., Weiss, R., Dubourg, V., Vanderplas, J., Passos, A., Cournapeau, D., Brucher, M., Perrot, M., and Duchesnay, E. (2011). Scikit-learn: Machine learning in Python. *Journal of Machine Learning Research*, 12:2825–2830.

Ragonneau, T. M. (2022). *Model-Based Derivative-Free Optimization Methods and Software*. PhD thesis, Department of Applied Mathematics, The Hong Kong Polytechnic University, Hong Kong.

Rousseeuw, P. J. (1984). Least median of squares regression. *Journal of the American Statistical Association*, 79(388):871–880.

Rousseeuw, P. J. and Van Driessen, K. (1999). A fast algorithm for the minimum covariance determinant estimator. *Technometrics*, 41(3):212–223.

Shimizu, S., Hoyer, P. O., Hyvärinen, A., Kerminen, A., and Jordan, M. (2006). A linear non-gaussian acyclic model for causal discovery. *Journal of Machine Learning Research*, 7(10).

Székely, G. J. and Rizzo, M. L. (2023). *The Energy of Data and Distance Correlation*. Chapman and Hall/CRC.

Székely, G. J., Rizzo, M. L., and Bakirov, N. K. (2007). Measuring and testing dependence by correlation of distances. *The Annals of Statistics*, 35(6):2769–2794.

Tharwat, A. (2021). Independent component analysis: An introduction. *Applied Computing and Informatics*, 17(2):222–249.

van der Walt, S., Schönberger, J. L., Nunez-Iglesias, J., Boulogne, F., Warner, J. D., Yager, N., Gouillart, E., Yu, T., and the scikit-image contributors (2014). scikit-image: image processing in Python. *PeerJ*, 2:e453, <https://doi.org/10.7717/peerj.453>.

Virtanen, P., Gommers, R., Oliphant, T. E., Haberland, M., Reddy, T., Cournapeau, D., et al. (2020). SciPy 1.0: Fundamental Algorithms for Scientific Computing in Python. *Nature Methods*, 17:261–272.

Voss, J., Belkin, M., and Rademacher, L. (2015). Optimal Recovery in Noisy ICA. *arXiv preprint arXiv:1612.05445*.

Supplementary Material

A Proofs of the propositions in Section 4

A.1 Proof of Proposition 1

To prove this proposition, we first generalize Lemmas A.1-A.3 of Matteson and Tsay (2017) to the lemmas below.

Lemma 1. $\forall \boldsymbol{\theta} \in \Theta :$

$$\sum_{k=1}^{d-1} d\text{Cor}_n(\psi(\mathbf{S}_{n,k}(\boldsymbol{\theta})), \psi(\mathbf{S}_{n,k_+}(\boldsymbol{\theta}))) \xrightarrow{a.s.} \sum_{k=1}^{d-1} d\text{Cor}(\psi(\mathbf{S}_k(\boldsymbol{\theta})), \psi(\mathbf{S}_{k_+}(\boldsymbol{\theta}))) \text{ for } n \rightarrow \infty.$$

Proof. Note that

$$\begin{aligned} & \left| \sum_{k=1}^{d-1} d\text{Cor}_n(\psi(\mathbf{S}_{n,k}(\boldsymbol{\theta})), \psi(\mathbf{S}_{n,k_+}(\boldsymbol{\theta}))) - \sum_{k=1}^{d-1} d\text{Cor}(\psi(\mathbf{S}_k(\boldsymbol{\theta})), \psi(\mathbf{S}_{k_+}(\boldsymbol{\theta}))) \right| \\ & \leq \sum_{k=1}^{d-1} |d\text{Cor}_n(\psi(\mathbf{S}_{n,k}(\boldsymbol{\theta})), \psi(\mathbf{S}_{n,k_+}(\boldsymbol{\theta}))) - d\text{Cor}(\psi(\mathbf{S}_k(\boldsymbol{\theta})), \psi(\mathbf{S}_{k_+}(\boldsymbol{\theta})))|. \end{aligned}$$

Here we know that $\psi(\mathbf{S}_k(\boldsymbol{\theta}))$ and $\psi(\mathbf{S}_{k_+}(\boldsymbol{\theta}))$ have finite moments $\forall k \in \{1, \dots, d-1\}$ as ψ is bounded. Hence we can use Corollary 1 of Székely et al. (2007) which states that $d\text{Cor}_n(\mathbf{X}_n, \mathbf{Y}_n)$ converges almost surely to $d\text{Cor}(\mathbf{X}, \mathbf{Y})$, establishing the lemma. \square

Next, we consider the group of all $d \times d$ orthogonal matrices with determinant 1, which is denoted by $\mathcal{SO}(d)$. On this group, take a pseudometric \mathcal{D} such that $\forall \mathbf{U}, \mathbf{A} \in \mathcal{SO}(d) : \mathcal{D}(\mathbf{U}, \mathbf{A}) \geq 0$, and $\mathcal{D}(\mathbf{U}, \mathbf{A}) = 0 \iff \exists \mathbf{P}$, a signed permutation matrix, such that $\mathbf{U} = \mathbf{PA}$. This yields equivalence classes on $\mathcal{SO}(d)$ where two elements are in the same equivalence class if and only if their distance is zero. This results is the quotient space $\mathcal{SO}(d)/\mathcal{D} = \mathcal{SO}(d)/\mathcal{D}$ of these equivalence classes with $\mathbf{U} = \mathbf{A}$ in $\mathcal{SO}(d)/\mathcal{D} \iff \mathcal{D}(\mathbf{U}, \mathbf{A}) = 0$.

Lemma 2. *The function $\mathcal{J}_n(\boldsymbol{\theta}) = \sum_{k=1}^{d-1} d\text{Cor}_n(\psi(\mathbf{S}_{n,k}(\boldsymbol{\theta})), \psi(\mathbf{S}_{n,k_+}(\boldsymbol{\theta})))$ is Lipschitz continuous in $\boldsymbol{\theta} : \mathbf{U}(\boldsymbol{\theta}) \in \mathcal{SO}(d)_{\mathcal{D}}$.*

Proof. First note that the bowl transform is Lipschitz continuous as it is continuously differentiable with bounded derivatives. Additionally, compositions of Lipschitz continuous functions remain Lipschitz continuous. Therefore, the only relevant difference with the proof of the similar Lemma A.2 in Matteson and Tsay (2017) is our use of $d\text{Cor}_n$ instead of $d\text{Cov}_n$. So for our Lemma to hold, we need to show that $d\text{Cor}_n$ is also Lipschitz continuous in our setting.

For this we check whether it has a bounded first derivative. We can use the quotient rule for this:

$$\begin{aligned} \frac{d}{d\boldsymbol{\theta}}(d\text{Cor}_n(\psi(\mathbf{S}_{n,k}(\boldsymbol{\theta})), \psi(\mathbf{S}_{n,k_+}(\boldsymbol{\theta})))) &= \frac{d}{d\boldsymbol{\theta}} \left(\frac{d\text{Cov}_n(\psi(\mathbf{S}_{n,k}(\boldsymbol{\theta})), \psi(\mathbf{S}_{n,k_+}(\boldsymbol{\theta})))}{\sqrt{d\text{Var}_n(\psi(\mathbf{S}_{n,k}(\boldsymbol{\theta})))d\text{Var}_n(\psi(\mathbf{S}_{n,k_+}(\boldsymbol{\theta})))}} \right) \\ &= \frac{\frac{d}{d\boldsymbol{\theta}}(d\text{Cov}_n(\psi(\mathbf{S}_{n,k}(\boldsymbol{\theta})), \psi(\mathbf{S}_{n,k_+}(\boldsymbol{\theta}))))}{d\text{Std}_n(\psi(\mathbf{S}_{n,k}(\boldsymbol{\theta})))d\text{Std}_n(\psi(\mathbf{S}_{n,k_+}(\boldsymbol{\theta})))} \\ &\quad - \left(\frac{\frac{d}{d\boldsymbol{\theta}}(d\text{Var}_n(\psi(\mathbf{S}_{n,k}(\boldsymbol{\theta}))))}{2d\text{Var}_n(\psi(\mathbf{S}_{n,k}(\boldsymbol{\theta})))} + \frac{\frac{d}{d\boldsymbol{\theta}}(d\text{Var}_n(\psi(\mathbf{S}_{n,k_+}(\boldsymbol{\theta}))))}{2d\text{Var}_n(\psi(\mathbf{S}_{n,k_+}(\boldsymbol{\theta})))} \right) d\text{Cor}_n(\psi(\mathbf{S}_{n,k}(\boldsymbol{\theta})), \psi(\mathbf{S}_{n,k_+}(\boldsymbol{\theta}))). \end{aligned} \quad (\text{A.1})$$

- The numerators are all bounded as $d\text{Cov}_n$ and $d\text{Var}_n$ are Lipschitz continuous in $\boldsymbol{\theta}$ (Matteson and Tsay, 2017), ψ is Lipschitz, and $d\text{Cor}_n$ is bounded by 1.
- For the denominators we need a lower bound to upper bound the whole expression in (A.1). For this we use the extreme value theorem that states that if a function is continuous on a closed and bounded interval that it attains its minimum. We apply this to

$$\begin{aligned} m_1 &= \min_{\ell \subseteq \{1, 2, \dots, d\}} \min_{\boldsymbol{\theta} \in [0, 2\pi]} d\text{Std}_n(\psi(\mathbf{S}_{n,\ell}(\boldsymbol{\theta}))) \\ m_2 &= \min_{\ell \subseteq \{1, 2, \dots, d\}} \min_{\boldsymbol{\theta} \in [0, 2\pi]} d\text{Var}_n(\psi(\mathbf{S}_{n,\ell}(\boldsymbol{\theta}))) \end{aligned}$$

so m_1 and m_2 exist. Additionally we have that $m_1, m_2 \geq 0$ are zero if and only if every sample observation in $\psi(\mathbf{S}_{n,\ell}(\boldsymbol{\theta}))$ is identical (Theorem 12.2 in Székely and Rizzo (2023)), an event that happens with probability zero in the ICA setting (note that ψ is a bijection). Hence we obtain fixed $m_1, m_2 > 0$ and we can use these to lower bound the denominators of (A.1). Therefore Equation (A.1) is upper bounded, and hence $d\text{Cor}_n$ is Lipschitz continuous in $\boldsymbol{\theta}$ as it has a bounded first derivative.

This finishes the proof of Lemma 2. □

Lemma 3. For $\mathcal{J}(\boldsymbol{\theta}) = \sum_{k=1}^{d-1} d\text{Cor}(\psi(\mathbf{S}_k(\boldsymbol{\theta})), \psi(\mathbf{S}_{k+}(\boldsymbol{\theta})))$ it holds that

$$\sup_{\boldsymbol{\theta}: \mathbf{U}(\boldsymbol{\theta}) \in \mathcal{SO}(d)} |\mathcal{J}_n(\boldsymbol{\theta}) - \mathcal{J}(\boldsymbol{\theta})| \xrightarrow{a.s.} 0 \quad \text{as } n \rightarrow \infty.$$

Proof. We proceed as in Matteson and Tsay (2017). In their proof they use the Arzelá-Ascoli theorem and the result of Lemma 1 to conclude that it is sufficient to show that

$$\lim_{c \rightarrow \infty} \overline{\lim}_n m_{\frac{1}{c}}(\mathcal{J}_n) \xrightarrow{a.s.} 0,$$

where

$$m_{\frac{1}{c}}(\mathcal{J}_n) = \sup\{|\mathcal{J}_n(\boldsymbol{\theta}) - \mathcal{J}_n(\boldsymbol{\phi})| : \mathbf{U}(\boldsymbol{\theta}), \mathbf{U}(\boldsymbol{\phi}) \in \mathcal{SO}(d), \|\mathbf{U}(\boldsymbol{\theta}) - \mathbf{U}(\boldsymbol{\phi})\|_F < 1/c\}.$$

Their proof centers around bounding $|\mathcal{J}_n(\boldsymbol{\theta}) - \mathcal{J}_n(\boldsymbol{\phi})|$ for $\boldsymbol{\theta}, \boldsymbol{\phi} \in \Theta$. They find the following (without transforming the random variables, and using $d\text{Cov}_n$ instead of $d\text{Cor}_n$):

$$|\mathcal{J}_n(\boldsymbol{\theta}) - \mathcal{J}_n(\boldsymbol{\phi})| \leq 4 \sum_{\ell=1}^{d-1} \left(\frac{2}{n} \sum_{i=1}^n \|\mathbf{s}_i(\boldsymbol{\theta}) - \mathbf{s}_i(\boldsymbol{\phi})\| \right) \times \\ \left(\binom{n}{2}^{-1} \sum_{i < j} \|\mathbf{s}_i(\boldsymbol{\theta}) - \mathbf{s}_j(\boldsymbol{\theta})\| + \binom{n}{2}^{-1} \sum_{i < j} \|\mathbf{s}_i(\boldsymbol{\phi}) - \mathbf{s}_j(\boldsymbol{\phi})\| \right)$$

Using the bowl transform does not alter the form of this upper bound, but using $d\text{Cor}_n$ does. Every observation is scaled, and we end up with an upper bound of the following form:

$$4 \sum_{\ell=1}^{d-1} \left(\underbrace{\frac{2}{n} \sum_{i=1}^n \left\| \frac{\psi(\mathbf{s}_i(\boldsymbol{\theta}))}{\sigma_n^{(\ell)}(\boldsymbol{\theta})} - \frac{\psi(\mathbf{s}_i(\boldsymbol{\phi}))}{\sigma_n^{(\ell)}(\boldsymbol{\phi})} \right\|}_{(1)} \right) \times \\ \left(\underbrace{\frac{1}{\sigma_n^{(\ell)}(\boldsymbol{\theta})} \binom{n}{2}^{-1} \sum_{i < j} \|\psi(\mathbf{s}_i(\boldsymbol{\theta})) - \psi(\mathbf{s}_j(\boldsymbol{\theta}))\| + \frac{1}{\sigma_n^{(\ell)}(\boldsymbol{\phi})} \binom{n}{2}^{-1} \sum_{i < j} \|\psi(\mathbf{s}_i(\boldsymbol{\phi})) - \psi(\mathbf{s}_j(\boldsymbol{\phi}))\|}_{(2)} \right) \quad (\text{A.2})$$

where

$$\sigma_n^{(\ell)}(\boldsymbol{\theta}) = \sqrt{\text{dVar}_n(\psi(\mathbf{S}_{n,\ell}(\boldsymbol{\theta}))) \text{dVar}_n(\psi(\mathbf{S}_{n,\ell+}(\boldsymbol{\theta})))}, \\ \sigma_n^{(\ell)}(\boldsymbol{\phi}) = \sqrt{\text{dVar}_n(\psi(\mathbf{S}_{n,\ell}(\boldsymbol{\phi}))) \text{dVar}_n(\psi(\mathbf{S}_{n,\ell+}(\boldsymbol{\phi})))}.$$

To bound the second factor (2) of Equation (A.2), we use the following:

- $\left[\binom{n}{2}^{-1} \sum_{i < j} \|\psi(\mathbf{s}_i(\boldsymbol{\theta})) - \psi(\mathbf{s}_j(\boldsymbol{\theta}))\| \right] \xrightarrow{a.s.} \mathbb{E}\|\psi(\mathbf{s}(\boldsymbol{\theta})) - \psi(\mathbf{s}'(\boldsymbol{\theta}))\|$ and
 $\left[\binom{n}{2}^{-1} \sum_{i < j} \|\psi(\mathbf{s}_i(\boldsymbol{\phi})) - \psi(\mathbf{s}_j(\boldsymbol{\phi}))\| \right] \xrightarrow{a.s.} \mathbb{E}\|\psi(\mathbf{s}(\boldsymbol{\phi})) - \psi(\mathbf{s}'(\boldsymbol{\phi}))\|$
by the SLLN for U-statistics and the boundedness of ψ .
- If we define $\sigma^{(\ell)}(\boldsymbol{\theta}) = \sqrt{\text{dVar}(\psi(\mathbf{S}_\ell(\boldsymbol{\theta}))) \text{dVar}(\psi(\mathbf{S}_{\ell+}(\boldsymbol{\theta})))}$, then we have $\sigma_n^{(\ell)}(\boldsymbol{\theta}) \xrightarrow{a.s.} \sigma^{(\ell)}(\boldsymbol{\theta})$ and $\sigma_n^{(\ell)}(\boldsymbol{\phi}) \xrightarrow{a.s.} \sigma^{(\ell)}(\boldsymbol{\phi})$ by almost sure convergence of the distance covariance (Székely et al., 2007) and the continuous mapping theorem. Here $\sigma^{(\ell)}(\boldsymbol{\theta})$ and $\sigma^{(\ell)}(\boldsymbol{\phi})$ are strictly greater than zero if the random variables are not degenerate, which is satisfied in the ICA setting.
- Hence (2) converges to

$$\frac{\mathbb{E}\|\psi(\mathbf{s}(\boldsymbol{\theta})) - \psi(\mathbf{s}'(\boldsymbol{\theta}))\|}{\sigma^{(\ell)}(\boldsymbol{\theta})} + \frac{\mathbb{E}\|\psi(\mathbf{s}(\boldsymbol{\phi})) - \psi(\mathbf{s}'(\boldsymbol{\phi}))\|}{\sigma^{(\ell)}(\boldsymbol{\phi})} > 0$$

which behaves well and is bounded.

To bound the first factor (1), we proceed as follows:

$$\begin{aligned} \frac{2}{n} \sum_{i=1}^n \left\| \frac{\psi(\mathbf{s}_i(\boldsymbol{\theta}))}{\sigma_n^{(\ell)}(\boldsymbol{\theta})} - \frac{\psi(\mathbf{s}_i(\boldsymbol{\phi}))}{\sigma_n^{(\ell)}(\boldsymbol{\phi})} \right\| &= \frac{2}{n} \sum_{i=1}^n \left\| \frac{\psi(\mathbf{s}_i(\boldsymbol{\theta}))}{\sigma_n^{(\ell)}(\boldsymbol{\theta})} - \frac{\psi(\mathbf{s}_i(\boldsymbol{\phi}))}{\sigma_n^{(\ell)}(\boldsymbol{\theta})} + \frac{\psi(\mathbf{s}_i(\boldsymbol{\phi}))}{\sigma_n^{(\ell)}(\boldsymbol{\theta})} - \frac{\psi(\mathbf{s}_i(\boldsymbol{\phi}))}{\sigma_n^{(\ell)}(\boldsymbol{\phi})} \right\| \\ &\leq \frac{1}{\sigma_n^{(\ell)}(\boldsymbol{\theta})} \underbrace{\frac{2}{n} \sum_{i=1}^n \|\psi(\mathbf{s}_i(\boldsymbol{\theta})) - \psi(\mathbf{s}_i(\boldsymbol{\phi}))\|}_{(1.a)} + \underbrace{\frac{2 \frac{1}{n} \sum_{i=1}^n \|\psi(\mathbf{s}_i(\boldsymbol{\phi}))\|}{\sigma_n^{(\ell)}(\boldsymbol{\theta}) \sigma_n^{(\ell)}(\boldsymbol{\phi})} |\sigma_n^{(\ell)}(\boldsymbol{\phi}) - \sigma_n^{(\ell)}(\boldsymbol{\theta})|}_{(1.b)} \end{aligned}$$

- The factor (1.a) has the same form as the factors in Matteson and Tsay (2017), where they show that it shrinks to zero for $\|\mathbf{U}(\boldsymbol{\theta}) - \mathbf{U}(\boldsymbol{\phi})\|$ going to zero.
- For (1.b), $\frac{\frac{1}{n} \sum_{i=1}^n \|\psi(\mathbf{s}_i(\boldsymbol{\phi}))\|}{\sigma_n^{(\ell)}(\boldsymbol{\theta}) \sigma_n^{(\ell)}(\boldsymbol{\phi})}$ behaves well as before, and converges to a constant. We however have to check that $|\sigma_n^{(\ell)}(\boldsymbol{\phi}) - \sigma_n^{(\ell)}(\boldsymbol{\theta})|$ goes to zero for $\|\mathbf{U}(\boldsymbol{\theta}) - \mathbf{U}(\boldsymbol{\phi})\|$ going to zero:

$$\begin{aligned} |\sigma_n^{(\ell)}(\boldsymbol{\theta}) - \sigma_n^{(\ell)}(\boldsymbol{\phi})| &= \left| \sqrt{\text{dVar}_n(\psi(\mathbf{S}_{n,\ell}(\boldsymbol{\theta}))) \text{dVar}_n(\psi(\mathbf{S}_{n,\ell+}(\boldsymbol{\theta})))} \right. \\ &\quad \left. - \sqrt{\text{dVar}_n(\psi(\mathbf{S}_{n,\ell}(\boldsymbol{\phi}))) \text{dVar}_n(\psi(\mathbf{S}_{n,\ell+}(\boldsymbol{\phi})))} \right| \\ &\leq \sqrt{\text{dVar}_n(\psi(\mathbf{S}_{n,\ell}(\boldsymbol{\theta})))} \left| \sqrt{\text{dVar}_n(\psi(\mathbf{S}_{n,\ell+}(\boldsymbol{\theta})))} - \sqrt{\text{dVar}_n(\psi(\mathbf{S}_{n,\ell+}(\boldsymbol{\phi})))} \right| \\ &\quad + \sqrt{\text{dVar}_n(\psi(\mathbf{S}_{n,\ell+}(\boldsymbol{\phi})))} \left| \sqrt{\text{dVar}_n(\psi(\mathbf{S}_{n,\ell}(\boldsymbol{\theta})))} - \sqrt{\text{dVar}_n(\psi(\mathbf{S}_{n,\ell}(\boldsymbol{\phi})))} \right| \end{aligned}$$

Here the factors $\sqrt{\text{dVar}_n(\psi(\mathbf{S}_{n,\ell}(\boldsymbol{\theta})))}$ and $\sqrt{\text{dVar}_n(\psi(\mathbf{S}_{n,\ell+}(\boldsymbol{\phi})))}$ behave well and converge to a positive constant. For the factor $\left| \sqrt{\text{dVar}_n(\psi(\mathbf{S}_{n,\ell}(\boldsymbol{\theta})))} - \sqrt{\text{dVar}_n(\psi(\mathbf{S}_{n,\ell}(\boldsymbol{\phi})))} \right|$

and the other similar factor we have

$$\begin{aligned} & \left| \sqrt{\text{dVar}_n(\psi(\mathbf{S}_{n,\ell}(\boldsymbol{\theta})))} - \sqrt{\text{dVar}_n(\psi(\mathbf{S}_{n,\ell}(\boldsymbol{\phi})))} \right| \\ &= \frac{\left| \text{dVar}_n(\psi(\mathbf{S}_{n,\ell}(\boldsymbol{\theta}))) - \text{dVar}_n(\psi(\mathbf{S}_{n,\ell}(\boldsymbol{\phi}))) \right|}{\left| \sqrt{\text{dVar}_n(\psi(\mathbf{S}_{n,\ell}(\boldsymbol{\theta})))} + \sqrt{\text{dVar}_n(\psi(\mathbf{S}_{n,\ell}(\boldsymbol{\phi})))} \right|}, \end{aligned}$$

where the denominator behaves well. For the numerator we can use the result of Lemma A.3 of Matteson and Tsay (2017), stating that this shrinks to zero when $\|\mathbf{U}(\boldsymbol{\theta}) - \mathbf{U}(\boldsymbol{\phi})\|$ goes to zero.

Putting this together, (1) shrinks to zero, and hence also the initial Equation (A.2):

$$\sup_{\|\mathbf{U}(\boldsymbol{\theta}) - \mathbf{U}(\boldsymbol{\phi})\|_F < \delta} |\mathcal{J}_n(\boldsymbol{\theta}) - \mathcal{J}_n(\boldsymbol{\phi})| \leq \alpha \delta$$

for some constant α .

With this result, we can, as in Matteson and Tsay (2017), apply the Arzelá-Ascoli theorem as $\mathcal{SO}(d)_D$ is separable, which yields:

$$\sup_{\boldsymbol{\theta}: \mathbf{U}(\boldsymbol{\theta}) \in \mathcal{SO}(d)_D} |\mathcal{J}_n(\boldsymbol{\theta}) - \mathcal{J}(\boldsymbol{\theta})| \xrightarrow{a.s.} 0 \quad \text{for } n \rightarrow \infty.$$

□

Proof of Proposition 1. Using these three extended lemmas, we can now prove Proposition 1. First note that $\forall n$ we have $\mathcal{J}_n(\boldsymbol{\theta}_0) \geq \mathcal{J}_n(\hat{\boldsymbol{\theta}}_n)$ and $\mathcal{J}(\hat{\boldsymbol{\theta}}_n) \geq \mathcal{J}(\boldsymbol{\theta}_0)$ because $\hat{\boldsymbol{\theta}}_n$ is the minimum of \mathcal{J}_n and $\boldsymbol{\theta}_0$ is the minimum of \mathcal{J} . This yields

$$\mathcal{J}_n(\boldsymbol{\theta}_0) - \mathcal{J}(\boldsymbol{\theta}_0) \geq \mathcal{J}_n(\hat{\boldsymbol{\theta}}_n) - \mathcal{J}(\boldsymbol{\theta}_0) \geq \mathcal{J}_n(\hat{\boldsymbol{\theta}}_n) - \mathcal{J}(\hat{\boldsymbol{\theta}}_n).$$

Therefore:

$$\begin{aligned} |\mathcal{J}_n(\hat{\boldsymbol{\theta}}_n) - \mathcal{J}(\boldsymbol{\theta}_0)| &\leq \max\{|\mathcal{J}_n(\boldsymbol{\theta}_0) - \mathcal{J}(\boldsymbol{\theta}_0)|, |\mathcal{J}_n(\hat{\boldsymbol{\theta}}_n) - \mathcal{J}(\hat{\boldsymbol{\theta}}_n)|\} \\ &\leq \sup_{\boldsymbol{\phi}: \mathbf{U}(\boldsymbol{\phi}) \in \mathcal{SO}(d)_D} |\mathcal{J}_n(\boldsymbol{\phi}) - \mathcal{J}(\boldsymbol{\phi})|. \end{aligned}$$

Now Lemma 3 states that this supremum goes to zero almost surely, hence $\mathcal{J}_n(\hat{\boldsymbol{\theta}}_n) \xrightarrow{a.s.} \mathcal{J}(\boldsymbol{\theta}_0)$ for $n \rightarrow \infty$. Additionally, we have that $\mathcal{SO}(d)_D$ is compact, therefore the minima of \mathcal{J} and \mathcal{J}_n exist in $\mathcal{SO}(d)_D$. Also, the argmin mapping is continuous, yielding $\mathbf{U}(\hat{\boldsymbol{\theta}}_n) \xrightarrow{a.s.} \mathbf{U}(\boldsymbol{\theta}_0)$ for $n \rightarrow \infty$ and $\mathbf{U}(\boldsymbol{\theta}_0) \in \mathcal{SO}(d)_D$. If now $\boldsymbol{\theta}_0$ is in $\bar{\Theta}$, a sufficiently large compact subset of Θ , the continuous mapping theorem gives us $\hat{\boldsymbol{\theta}}_n \xrightarrow{a.s.} \boldsymbol{\theta}_0$. □

A.2 Proof of Proposition 2

We follow the lines of Theorem 2.2 of Matteson and Tsay (2017).

We use the following subset Ω of $\mathcal{SO}(d)$ introduced by Chen and Bickel (2005). First, each row of \mathbf{U} has Euclidean norm 1. Second, the element with maximal modulus in each row of \mathbf{U} is positive. Finally, the rows of \mathbf{U} are sorted according to the partial order \prec that is given by: $\forall a, b \in \mathbb{R}^d$, $a \prec b$ if and only if there exists $k \in \{1, \dots, d\}$ such that $a_k < b_k$ and $a_j = b_j$ for $j \in \{1, \dots, k-1\}$. This construction gets rid of identifiability issues as each \mathbf{U} along with all of its signed permutations corresponds to a single element in Ω .

Now we introduce a path γ between two points on the unit ball in \mathbb{R}^d following Matteson and Tsay (2017). Consider a unit ball in \mathbb{R}^d centered at A , which contains the points B and C , and let the angle $\xi > 0$ denote the smallest value such that $\cos(\xi) = \langle \vec{AB}, \vec{AC} \rangle$. For $\tau \in \mathbb{R}$, let

$$\gamma(\tau) = \cos(\tau)\vec{AB} + \sin(\tau)\vec{AD}$$

denote a path from \vec{AB} to \vec{AC} , in which \vec{AD} is a unit tangent vector at B such that \vec{AB} , \vec{AC} , and \vec{AD} are on the same hyperplane. Then, $\gamma(0) = B$, $\gamma(\xi) = C$, and

$$\left\| \frac{\partial}{\partial \tau} \gamma(\tau) \right\| = 1; \quad \text{further, } \|\gamma(\tau_2) - \gamma(\tau_1)\| \leq |\tau_2 - \tau_1|.$$

By definition, each row of $\mathbf{U} \in \Omega$ is on the unit ball in \mathbb{R}^d . Let ξ_1, \dots, ξ_d denote the angles between the corresponding rows of $\mathbf{U}_0 = \mathbf{U}_{\theta_0}$ and $\widehat{\mathbf{U}} = \mathbf{U}_{\hat{\theta}_n}$.

Let $\hat{\eta} = \sqrt{\sum_{k=1}^d \xi_k^2}$, and note that $\|\widehat{\mathbf{U}} - \mathbf{P}_{\pm} \mathbf{U}_0\| = o_p(1)$ implies $\hat{\eta} = o_p(1)$.

Now let $\gamma : \mathbb{R} \rightarrow \mathbb{R}^{d \times d}$ be such that $\gamma(0) = \mathbf{U}_0$ and $\gamma(\hat{\eta}) = \widehat{\mathbf{U}}$, by considering $\gamma(\cdot)$ for the k th rows, as described above but rescaled by $\xi_k/\hat{\eta}$. Then we similarly note that

$$\left\| \frac{\partial}{\partial \tau} \gamma(\tau) \right\| = \sqrt{\sum_{k=1}^d \left(\frac{\xi_k}{\hat{\eta}} \right)^2} = 1, \quad \text{and } \|\gamma(\tau_2) - \gamma(\tau_1)\| \leq |\tau_2 - \tau_1|.$$

As such, for $\|\widehat{\mathbf{U}} - \mathbf{P}_{\pm} \mathbf{U}_0\| \leq \hat{\eta}$ and sufficiently small $\tau \geq 0$, we note $\gamma(\tau) \in \Omega$.

We will now use $\mathcal{J}_n(\gamma(\tau))$ to characterize the objective function, where $\gamma(0) = \mathbf{U}_0$ and $\gamma(\hat{\eta}) = \widehat{\mathbf{U}}$. We consider

$$\mathcal{J}_n(\gamma(\tau)) = \sum_{k=1}^{d-1} \text{dCor}_n(\psi(\mathbf{S}_{n,k}(\gamma(\tau))), \psi(\mathbf{S}_{n,k+}(\gamma(\tau)))) .$$

Now we consider the first derivative of this objective with respect to τ , $\frac{\partial}{\partial \tau} \mathcal{J}_n(\gamma(\tau))$ and use Taylor's theorem with the mean-value theorem to conclude that there exists a $\bar{\tau} \in [0, \hat{\eta}]$ for which

$$0 = \frac{\partial}{\partial \tau} \mathcal{J}_n(\gamma(\hat{\eta})) = \frac{\partial}{\partial \tau} \mathcal{J}_n(\gamma(0)) + \hat{\eta} \frac{\partial^2}{\partial \tau^2} \mathcal{J}_n(\gamma(\bar{\tau})),$$

which implies

$$\hat{\eta} = -\frac{\frac{\partial}{\partial \tau} \mathcal{J}_n(\gamma(0))}{\frac{\partial^2}{\partial \tau^2} \mathcal{J}_n(\gamma(\bar{\tau}))}.$$

First consider the numerator. We know \mathcal{J}_n consists of $d - 1$ distance correlations, each of which can be written as a distance covariance (i.e., a sum of three U-statistics) multiplied by a scale factor. The scale factor converges in probability to its population counterpart as a consequence of the continuous mapping theorem and the a.s. convergence of the distance variance obtained in Székely et al. (2007), and is thus $\mathcal{O}_P(1)$. The derivative of the scale term is also $\mathcal{O}_P(1)$. This follows from the chain rule, as the resulting expression is a continuous function of the scale itself, the distance variance, and the first derivative of the distance variance, all of which converge in probability to their population counterparts.

We can thus conclude that the scale factors do not affect the convergence rate. This leaves the derivative of the distance covariance and the distance covariance itself as deciding factors. The first is $\mathcal{O}_P(1/\sqrt{n})$ by Matteson and Tsay (2017), whereas the second is $\mathcal{O}_P(1/\sqrt{n})$ by Székely et al. (2007) under the model ICA assumptions. We conclude that each of the distance correlation terms in the numerator is $\mathcal{O}_P(1/\sqrt{n})$, and thus the numerator itself as well. Note that we can obtain a similar result under model misspecification provided that $\mathbb{E} [\frac{\partial}{\partial \tau} \mathcal{J}_n(\gamma(\tau))|_{\tau=0}] = o_P(1/\sqrt{n})$.

Now consider the denominator $\frac{\partial^2}{\partial \tau^2} \mathcal{J}_n(\gamma(\bar{\tau}))$. We need to show that this quantity is bounded from below asymptotically, so that it does not interfere with the $\mathcal{O}_P(1/\sqrt{n})$ convergence of the numerator. As $\mathcal{J}_n(\gamma(\bar{\tau}))$ is a sum of distance correlations, $\frac{\partial^2}{\partial \tau^2} \tilde{\mathcal{J}}_n(\gamma(\tau))$ depends on the distance covariances and their first two derivatives, as well as the scale factors and their first two derivatives. Note that all the involved quantities are stochastically bounded. Of the six terms coming out of the second derivative of each distance correlation, all but one contain either $d\text{Cov}_n$ or $d\text{Cov}'_n$, both of which converge to zero in probability under the ICA model. The final term is $\frac{\partial^2}{\partial \tau^2} d\text{Cov}_n(\gamma(\tau))$ multiplied by a scale factor. The scale factor

converges in probability to its population counterpart (which is a strictly positive number) by the continuous mapping theorem and Székely et al. (2007). The problem is therefore reduced to bounding the sum of the second derivatives of all dCov-terms from below, which was done in Matteson and Tsay (2017).

As a result, we obtain

$$\frac{\partial^2}{\partial \tau^2} \mathcal{J}_n(\gamma(\bar{\tau})) = \min_{\frac{\partial}{\partial \tau} \gamma(0), \frac{\partial^2}{\partial \tau^2} \gamma(0)} \frac{\partial^2}{\partial \tau^2} \mathcal{J}(\gamma(\tau)) + o_p(1),$$

where $\min_{\frac{\partial}{\partial \tau} \gamma(0), \frac{\partial^2}{\partial \tau^2} \gamma(0)} \frac{\partial^2}{\partial \tau^2} \mathcal{J}(\gamma(\tau)) > 0$ given that $\gamma(0)$ is the unique global minimizer and by differentiability and compactness. Putting the results for the numerator and the denominator together, we obtain

$$\hat{\eta} = \mathcal{O}_P(n^{-1/2}).$$

This ends the proof.

B Tables with detailed results of Section 5.2

B.1 Uncontaminated data

	RICA	RICA no sweeps	dCovICA	FastICA	Infomax	JADE	RADICAL
a	11.57	11.52	2.66	5.24	2.57	3.71	4.15
b	6.04	6.03	2.67	3.89	2.94	4.83	4.10
c	5.01	5.05	1.78	2.36	2.06	1.74	2.93
d	16.08	16.01	4.93	5.35	4.17	5.46	7.44
e	3.80	3.80	1.55	6.53	3.70	4.17	2.83
f	1.69	1.69	1.41	2.02	1.73	2.55	4.08
g	2.29	2.29	1.53	1.73	1.58	1.64	5.01
h	10.37	10.33	4.14	4.14	4.01	4.44	8.59
i	17.31	17.42	8.24	7.51	6.69	7.17	20.93
j	3.77	3.77	1.63	50.55	46.81	6.94	3.59
k	4.58	4.58	2.32	41.36	36.52	14.84	4.47
l	5.28	5.28	4.20	38.01	35.25	26.53	8.44
m	3.13	4.24	28.90	6.44	4.81	3.32	1.98
n	8.22	9.27	14.22	41.28	45.85	12.10	4.93
o	9.54	9.53	8.59	8.36	7.08	4.80	13.18
p	2.45	2.45	1.84	20.44	14.37	3.73	2.76
q	8.06	8.66	7.84	16.83	23.49	42.86	6.14
r	12.48	12.58	8.32	43.23	44.99	24.99	20.58
mean	7.32	7.47	5.93	16.96	16.03	9.77	7.01

Table 1: Amari error ($\times 100$) for $d = 2$, no contamination.

	RICA	RICA no sweeps	dCovICA	FastICA	Infomax	JADE	RADICAL
a	10.27	10.53	2.77	2.36	2.48	3.97	3.87
b	5.85	5.85	4.74	2.95	3.03	4.77	4.19
c	3.87	4.42	8.19	2.09	2.08	1.83	2.15
d	14.72	15.53	6.58	4.50	4.21	5.57	7.58
e	2.71	2.70	1.70	4.03	3.52	4.15	2.35
f	2.33	10.16	16.49	1.73	1.78	2.57	1.86
g	2.59	9.28	12.20	1.54	1.54	1.61	2.09
h	8.57	9.32	12.13	4.10	4.12	4.62	13.64
i	17.41	19.74	18.80	6.34	6.84	7.15	35.48
j	2.68	3.75	3.38	28.04	26.46	9.20	2.15
k	3.21	5.83	2.73	30.10	29.58	17.87	3.64
l	5.17	8.05	4.48	37.13	36.89	34.21	9.57
m	11.29	16.20	26.61	6.05	4.85	3.47	6.64
n	28.95	35.99	41.21	40.94	42.12	18.40	30.64
o	15.41	19.17	23.32	7.52	6.81	4.78	35.22
p	3.26	12.54	10.05	18.64	14.64	3.93	2.19
q	19.24	26.57	33.87	22.18	33.24	45.75	27.90
r	14.22	19.02	16.52	41.28	41.66	32.70	35.32
mean	9.54	13.04	13.65	14.53	14.77	11.47	12.58

Table 2: Amari error ($\times 100$) for $d = 4$, no contamination.

	RICA	RICA no sweeps	dCovICA	FastICA	Infomax	JADE	RADICAL
a	6.69	7.14	1.91	1.68	1.65	2.81	2.67
b	3.86	3.77	5.64	2.00	2.08	3.36	2.95
c	1.70	7.52	13.67	1.49	1.41	1.26	1.34
d	9.71	11.47	5.42	2.86	2.75	4.14	5.10
e	2.00	2.01	1.18	2.86	2.41	2.98	1.63
f	1.61	16.33	17.25	1.18	1.21	1.72	1.33
g	1.83	16.36	15.94	1.07	1.06	1.11	1.40
h	4.75	12.15	19.15	2.73	2.75	3.19	13.36
i	14.80	21.88	26.49	4.61	4.45	5.08	37.00
j	1.91	7.14	6.50	18.43	16.96	5.09	1.86
k	2.23	10.22	5.18	24.38	22.06	14.03	2.75
l	3.67	10.16	5.29	32.63	32.28	29.77	6.29
m	13.28	18.03	25.63	3.84	3.36	2.45	15.98
n	36.86	38.46	39.15	37.49	36.89	11.61	36.46
o	12.48	20.11	22.65	5.33	4.96	3.49	37.46
p	1.99	18.06	16.46	12.31	8.95	2.69	1.50
q	30.41	34.45	35.57	17.54	30.49	41.89	33.53
r	12.37	24.65	20.19	39.62	39.37	29.65	37.69
mean	9.01	15.55	15.74	11.78	11.95	9.24	13.35

Table 3: Amari error ($\times 100$) for $d = 6$, no contamination.

B.2 Clustered contamination

	RICA	RICA no sweeps	dCovICA	FastICA	Infomax	JADE	RADICAL
a	7.77	7.96	54.98	80.17	77.88	64.78	85.76
b	4.51	4.45	55.78	84.11	83.43	84.71	84.87
c	2.71	2.71	56.72	85.45	84.43	86.64	87.35
d	15.65	14.36	56.04	83.35	82.20	81.16	85.62
e	3.51	3.51	55.00	85.41	85.13	84.44	3.32
f	1.83	1.83	57.00	85.36	84.45	86.41	3.99
g	1.89	1.89	57.04	84.91	84.07	86.06	9.52
h	22.27	21.85	56.60	85.09	84.11	86.36	87.04
i	38.91	37.82	56.54	85.34	84.37	86.35	86.98
j	5.96	5.96	56.30	86.24	85.56	86.85	7.15
k	3.91	3.91	56.18	85.14	84.21	85.81	77.49
l	5.22	5.32	56.28	85.28	84.42	86.27	86.08
m	8.28	10.54	56.58	85.39	84.41	86.50	87.30
n	22.63	21.57	56.39	85.45	84.46	86.83	87.13
o	25.79	24.16	56.46	85.16	84.15	86.44	87.04
p	2.91	3.43	56.48	85.29	84.28	86.40	84.84
q	16.82	16.31	56.25	84.88	84.04	86.12	86.32
r	14.14	13.65	56.28	85.22	84.26	86.41	86.97
mean	11.37	11.18	56.27	84.85	83.88	84.70	68.04

Table 4: Amari error ($\times 100$) for $d = 2$, clustered contamination.

	RICA	RICA no sweeps	dCovICA	FastICA	Infomax	JADE	RADICAL
a	10.74	16.16	35.13	41.39	38.48	33.83	44.67
b	4.58	12.20	36.11	42.33	41.35	43.36	45.11
c	16.76	25.71	36.47	42.98	41.94	45.24	47.63
d	18.36	19.73	37.22	43.29	41.98	41.90	46.06
e	2.60	2.77	31.55	41.88	41.10	43.52	43.60
f	5.73	26.60	37.17	42.65	41.23	45.44	51.37
g	2.40	19.04	35.53	41.88	40.70	44.90	51.20
h	49.50	49.57	38.95	43.42	42.40	45.64	52.02
i	50.92	49.21	40.78	45.11	44.89	47.38	52.98
j	2.95	5.72	32.74	47.89	46.19	45.37	33.39
k	3.17	7.28	34.18	48.71	46.95	46.45	44.63
l	6.41	12.28	35.82	49.60	48.92	49.34	47.93
m	47.02	46.79	40.37	43.77	42.60	44.96	51.78
n	32.46	31.90	44.84	50.30	49.44	50.54	54.41
o	47.39	47.17	41.67	45.86	44.43	46.62	55.84
p	5.60	17.57	36.36	47.57	45.89	46.32	49.42
q	23.72	28.59	43.22	50.07	48.81	52.24	54.90
r	26.28	29.54	38.95	52.11	51.35	51.09	53.04
mean	19.81	24.88	37.61	45.60	44.37	45.79	48.89

Table 5: Amari error ($\times 100$) for $d = 4$, clustered contamination.

	RICA	RICA no sweeps	dCovICA	FastICA	Infomax	JADE	RADICAL
a	11.04	17.12	24.35	26.69	25.17	21.39	29.33
b	3.15	14.18	25.82	27.67	26.75	28.25	29.60
c	37.03	40.71	28.05	27.57	26.83	29.91	30.52
d	15.01	19.14	26.49	27.90	27.13	27.28	30.02
e	1.89	3.05	22.23	26.32	27.45	26.89	28.93
f	38.34	41.02	35.23	27.48	26.51	30.09	32.30
g	30.99	38.41	32.91	26.90	25.61	29.90	31.11
h	45.29	47.98	32.85	28.65	27.85	30.15	40.48
i	45.40	46.18	36.18	30.02	29.35	31.56	46.36
j	1.98	10.18	25.85	35.90	36.47	29.51	26.87
k	2.30	14.04	26.05	41.84	41.59	31.32	29.52
l	6.50	21.74	26.94	42.80	42.32	37.15	35.31
m	43.36	46.10	34.10	29.20	28.39	29.85	47.41
n	38.88	38.45	40.42	44.45	42.86	38.75	49.84
o	43.53	45.88	36.08	30.06	29.27	30.25	47.85
p	22.04	29.43	30.21	32.22	30.55	30.13	35.94
q	29.76	33.02	41.23	42.74	43.90	47.23	48.76
r	31.53	32.70	33.48	44.99	44.34	42.24	47.38
mean	24.89	29.96	31.03	32.97	32.35	31.77	37.09

Table 6: Amari error ($\times 100$) for $d = 6$, clustered contamination.

B.3 Multiplicative contamination

	RICA	RICA no sweeps	dCovICA	FastICA	Infomax	JADE	RADICAL
a	10.14	10.12	65.34	64.88	74.03	75.99	30.45
b	6.07	6.11	88.35	75.43	83.39	84.03	67.03
c	30.39	30.54	3.25	41.03	45.07	86.88	9.03
d	18.46	18.52	78.89	72.30	80.26	81.45	69.82
e	2.20	2.20	11.32	34.18	22.31	22.13	2.60
f	5.83	5.88	31.51	84.60	85.86	85.79	3.30
g	6.04	6.04	3.80	45.84	57.41	86.60	8.16
h	19.53	19.52	92.78	83.37	85.78	85.85	84.30
i	22.60	22.49	92.55	83.94	85.80	86.04	84.42
j	4.08	4.08	2.65	84.43	85.65	85.17	2.42
k	3.73	3.73	5.82	82.60	85.26	85.44	13.00
l	5.24	5.24	81.62	81.91	85.33	85.70	82.66
m	49.17	49.75	94.41	85.16	86.24	86.34	5.60
n	16.96	19.24	93.27	83.41	85.78	86.11	84.36
o	29.93	30.29	93.10	83.98	85.63	86.12	84.58
p	3.56	3.88	77.66	85.44	86.54	86.68	2.90
q	8.78	9.88	92.74	81.52	85.24	85.85	84.52
r	10.67	11.57	92.13	82.53	85.57	85.98	84.41
mean	14.08	14.39	61.18	74.25	77.29	81.56	44.64

Table 7: Amari error ($\times 100$) for $d = 2$, multiplicative contamination.

	RICA	RICA no sweeps	dCovICA	FastICA	Infomax	JADE	RADICAL
a	7.92	9.22	38.87	41.97	47.73	54.20	7.53
b	4.96	5.36	50.90	45.70	55.36	59.78	19.52
c	3.04	3.64	58.33	60.30	64.11	63.49	29.31
d	12.91	15.06	46.97	44.14	54.09	58.61	30.14
e	3.05	2.98	11.53	30.48	20.40	34.25	2.48
f	2.07	5.18	50.29	52.92	59.82	61.95	1.98
g	2.03	3.99	50.56	59.48	62.63	62.34	2.13
h	8.70	11.55	57.37	51.47	58.63	62.77	51.82
i	19.71	23.14	56.67	50.63	59.29	62.70	54.12
j	2.91	4.26	20.44	52.00	58.87	59.23	2.54
k	3.41	6.49	43.83	50.55	58.22	60.06	11.33
l	5.69	9.65	52.27	50.12	58.07	60.97	48.80
m	10.21	13.86	57.63	53.04	59.37	62.58	41.67
n	35.50	40.34	57.19	52.17	60.05	64.87	53.52
o	14.84	18.29	56.40	51.62	59.62	63.85	54.22
p	3.35	11.92	56.45	52.32	59.08	62.43	22.59
q	30.71	33.76	56.16	49.95	57.66	62.36	52.23
r	18.12	23.57	55.09	50.01	58.07	62.28	52.39
mean	10.51	13.46	48.72	49.94	56.17	59.93	29.91

Table 8: Amari error ($\times 100$) for $d = 4$, multiplicative contamination.

	RICA	RICA no sweeps	dCovICA	FastICA	Infomax	JADE	RADICAL
a	6.63	9.08	37.17	40.26	44.52	49.63	4.94
b	3.71	6.40	46.26	41.86	51.30	56.25	12.84
c	1.82	8.01	51.31	47.13	54.28	57.63	42.22
d	9.41	15.49	42.69	40.86	49.01	53.10	24.38
e	2.27	2.23	15.21	29.37	20.17	36.65	1.71
f	4.36	20.62	47.26	44.13	52.59	56.90	2.10
g	1.71	15.61	49.33	47.05	53.38	58.12	1.65
h	27.62	31.20	49.18	43.38	52.75	57.69	47.20
i	39.89	39.45	49.93	44.24	53.56	57.44	47.08
j	1.99	8.39	39.51	44.15	51.14	54.92	2.04
k	2.36	12.01	46.43	44.37	50.78	55.45	12.44
l	5.07	18.26	47.30	43.50	52.47	56.64	42.88
m	23.73	27.44	50.09	44.49	53.89	58.30	47.99
n	39.54	40.70	50.11	43.86	52.76	57.52	46.35
o	33.12	34.27	50.29	43.89	53.38	57.57	47.31
p	5.50	21.64	50.19	45.32	53.50	57.59	43.04
q	32.56	35.54	49.30	43.74	53.36	58.54	46.78
r	27.27	31.39	48.86	44.20	52.92	57.78	46.56
mean	14.92	20.98	45.58	43.10	50.32	55.43	28.86

Table 9: Amari error ($\times 100$) for $d = 6$, multiplicative contamination.